Medium Access Control Protocol Design for In-Vehicle Power Line Communication

by

Amir Kenarsari Anhari

B.Sc., Sharif University of Technology, Iran, 2011

A THESIS SUBMITTED IN PARTIAL FULFILLMENT OF
THE REQUIREMENTS FOR THE DEGREE OF

MASTER OF APPLIED SCIENCE

in

The Faculty of Graduate and Postdoctoral Studies

(Electrical and Computer Engineering)

THE UNIVERSITY OF BRITISH COLUMBIA
(Vancouver)

October 2013

Abstract

Nowadays, the number of electronic devices in vehicles grows at an exponential rate. For the purpose of communication between these components, several standardized communication protocols such as controller area network (CAN), local interconnect network (LIN), and FlexRay have been developed and are used in vehicles. However, the use of additional wires for data communication still results in a significant increase in the complexity, volume, weight, and cost of wiring harness. Vehicular power line communication (V-PLC) is an interesting alternative that offers numerous advantages. This technology reuses the existing direct current (DC) power network in vehicles as the physical medium for data transmission and allows eliminating some of the wiring harnesses devoted to convey data signals. Hence, This technology can potentially reduce the vehicle cost, weight, and fuel consumption. However, to provide reliable communication over power lines, several challenges need to be addressed. These include impulsive noise produced by electrical devices connected to the bus and frequency-selective behavior of the power line channels introduced by impedance mismatches in the wiring harness.

In this thesis, we study research challenges for the medium access control (MAC) protocol design of V-PLC networks. We propose MAC protocols for such systems, which provide fast collision resolution, and perform performance evaluations on these protocols in terms of collision probability, system throughput, and packet delay. Our results show that these protocols outperform the previously proposed protocol, con-

tention detection and resolution (CDR) [1] in all scenarios.

We then investigate the effect of carrier sensing errors on the performance of the proposed MAC protocols. We start with addressing the problem of detection of unknown signals in impulsive noise by using a robust detector, which first removes the impulses from the signal and then performs linear signal detection on the cleaned samples. We obtain the network throughput and delay of the proposed protocols as a function of carrier sensing errors. We then suggest a framework for the optimal joint design of the physical layer signal detector and MAC layer protocol.

Preface

Hereby, I declare that I am the first author of this thesis. Chapters 3-5 are based on work that has been published or submitted for publication. The related publications were co-authored by Professor Victor C.M. Leung. The work in Chapter 4 was done in collaboration with Professor Lutz Lampe.

For all publications, I conducted the paper survey on related topics, performed the analysis, and carried out the simulations of the considered communication systems. The papers were originally prepared by me, and further revised by all the co-authors. The following publications are accomplished through this research.

Conference Papers

- Amir Kenarsari-Anhari, Victor C.M. Leung, and Lutz Lampe, "A Distributed MAC Protocol for In-Vehicle Power Line Communication under Imperfect Carrier Sensing," in *Proc of IEEE International Symposium on Personal, Indoor and Mobile Radio Communications (PIMRC)*, London, UK, September 2013.

- Amir Kenarsari-Anhari and Victor C.M. Leung, "Multi-Carrier Medium Access Control for In-Vehicle Power Line Communication with Imperfect Sensing," in *Proc of IEEE Vehicular Technology Conference (VTC Spring)*, Dresden, Germany, June 2013.

Table of Contents

List of Tables

List of Figures

List of Acronyms

ACK	Acknowledgment
ADC	Analog-to-Digital Converter
AWGN	Additive White Gaussian Noise
BPF	Band-pass Filter
CAN	Controller Area Network
CDF	Cumulative Distribution Function
CDMA	Code Division Multiple Access
CDR	Contention Detection and Resolution
CRC	Cyclic Redundancy Check
CSMA	Carrier Sense Multiple Access
CSMA/CA	Carrier Sense Multiple Access with Collision Avoidance
CSMA/CD	Carrier Sense Multiple Access with Collision Detection
DC	Direct Current
ECDF	Empirical Cumulative Distribution Function
ECU	Electronic Control Unit
ED	Energy Detection
FDMA	Frequency Division Multiple Access
IEEE	Institute of Electrical and Electronics Engineers
I.i.d.	Independent and Identically Distributed
LIN	Local Interconnect Network

MAC	Medium Access Control
Pdf	Probability Density Function
PHY	Physical layer
PLC	Power Line Communication
QoS	Quality of Service
ROC	Receiver Operating Characteristic
SNR	Signal-to-Noise Ratio
TDMA	Time Division Multiple Access
UART	Universal Asynchronous Receiver/Transmitter
V-PLC	Vehicular Power Line Communication

Acknowledgments

I would like to express my greatest gratitude to my supervisor, Professor Victor C.M. Leung, for his guidance and valuable advice throughout my graduate study.

I would also like to thank Professor Lutz Lampe for his helpful comments and assistance during the course of this work.

This work was supported by a grant from AUTO21 under the Canadian Network of Centres of Excellence Program.

Chapter 1

Introduction

The automotive industry introduces more and more electronic devices to ensure safety and comfort of occupants. There are several electronic control units (ECUs) to control the crucial on-board subsystems, such as ignition and braking systems. For the purpose of communication between ECUs, several standardized wire protocols such as CAN, LIN, and FlexRay were introduced and used in vehicles. However, each of these protocols requires its own dedicated communication lines which results in the increasingly complex network architectures, higher volume, weight and cost of the wiring harnesses [2]. V-PLC offers the advantage of using the existing power cables in vehicles for data transmissions, and therefore can significantly reduce the vehicle cost, weight, and fuel consumption.

The use of power line communication inside vehicles has attracted a lot of attentions from industry in a past few years. For instance, Yamar Electronics. Ltd. introduced the DC-BUS technology which enables the transfer of both data and power over a single cable [3]. They also designed several chips for the various applications supporting LIN, CAN, and universal asynchronous receiver/transmitter (UART) protocols to communicate over DC-BUS.

In order to fully exploit PLC technology in vehicles, MAC layer must be properly designed to provide reliable data transmission. We focus on random access MAC protocols which arbitrate the packet transmissions over power lines. The goal of the MAC protocol is to allow users to share a channel in an efficient manner by providing

a low collision rate, a high throughput, and a low delay average.

However, there are several challenges for deploying PLC system in vehicles that need to be considered while designing a MAC protocol for such a system. For instance, the measurements reported in [2, 4–6] confirm the frequency-selective behavior of V-PLC transmission channels. Another difficulty encountered in designing a PLC system for vehicles is the presence of non-stationary impulsive noise caused by various electrical devices connected to the V-PLC network [7]. Hence, in this thesis, we aim to investigate the effect of the carrier sensing errors on the performance of the MAC layer.

1.1 Motivations and Objectives

The related work on the design of a random access protocol for V-PLC network is limited. The authors in [1] proposed a random access protocol which resolves the contention by randomly switching between carrier sense and carrier transmission modes in each slot. They have calculated the collision probability by mathematical analysis with the assumption of perfect carrier sensing. On the contrary, as we mentioned before, measurements of V-PLC transmission channels indicate the presence of non-stationary impulsive noise. Hence, our work in this thesis, considers imperfect carrier sensing and also attempts to improve the MAC layer efficiency by including the physical layer parameters into the MAC layer design process. Our results also show that the proposed MAC protocols in this thesis outperform the MAC protocol in [1] significantly. We would like to remark that, to the best of our knowledge, the work in [1] is the only existing random access MAC protocol designed for V-PLC systems.

1.2 Contributions

We can summarize our contributions in this thesis as follows:

- We propose MAC protocols to provide random access over power line network. The first protocol uses multiple channels to arbitrate the packet transmission. The second protocol minimizes the contention between nodes in time by constructing a tournament between contending nodes, and the third protocol uses a combination of the techniques used in the design of the first two MAC protocols.
- We provide a mathematical framework for investigating the impact of carrier sensing errors on the performance of the proposed protocols.
- Based on the above framework, we design a communication system which provides better performance in terms of throughput and delay.

1.3 Structure of the Thesis

The rest of the thesis is organized as follows. In Chapter 2, we give an overview of the V-PLC system and present a summary of the related works. In addition, Chapter 2 covers the fundamentals of CAN protocol and carrier sensing. Chapter 3 introduces a frequency-domain collision resolution scheme that uses a combination of time and frequency multiplexing for resolving the contention between different devices connected to the harness. We also investigate the impact of carrier sensing errors on the performance of the proposed MAC protocol in Chapter 3. In Chapter 4, we introduce a time-domain collision resolution MAC protocol for V-PLC system and analyze its performance under imperfect carrier sensing errors. Chapter 5 introduces a multi-channel MAC protocol, which first resolves the contention over frequency

domain, and then resolves the contention by constructing a tournament scheme on each frequency channel. Chapter 6 outlines the main contributions of this thesis and describes possible future works.

Chapter 2

Background and Related Work

In this chapter, we first give an overview of the V-PLC system, followed by a description of the challenges in developing such a system. We then describe an automotive protocol, which is referred to as CAN protocol, used in vehicles for connecting ECUs. After that, we briefly describe the V-PLC MAC protocol reported in [1], which similar to CAN protocol, provides random access for data transmission in vehicles. Since we study MAC protocols under imperfect carrier sensing in Chapters 3-5, we introduce the basics of carrier sensing in this chapter as well.

2.1 Vehicular Power Line Communication

In the previous chapter, we have stated the benefits of using PLC technology in vehicles such as reducing the vehicle cost, weight, and fuel consumption. We also described a number of challenges that need to be addressed while designing a V-PLC system. V-PLC is much different from the PLC for home applications due to its complicated wiring topologies, transmission channel characteristics, attenuation, and noise. Therefore, special attention should be taken while designing such a system.

In the design and analysis of a conventional communication system, noise is usually modeled as additive white Gaussian noise (AWGN). However, the measurements [6–8] show that this model is not valid for V-PLC channels. The measurements of V-PLC system confirms that there are three types of noise in vehicles: (i) colored

background noise. (ii) narrow-band noise. (iii) impulsive noise. Knowledge of the noise characteristics is thus essential for optimizing the communication system, e.g., modulation schemes, channel codings, MAC protocols, etc.

2.2 Controller Area Network

The CAN bus is a serial communication bus in which all connected ECUs can send as well as receive messages. CAN bus was initially designed by Robert Bosch GmbH in the mid-1980s for multiplexing the increasing number of ECUs in cars and thus for decreasing the wire harnesses. Consequently, it became an open systems interconnection (OSI) standard in 1994 and is now a de facto standard in Europe for in-vehicle data transmission. Today, CAN is used as a society of automotive engineers (SAE) class C network in the power-train and chassis domains providing up to 1Mbps, but it also serves as a class B network with a bit rate up to 125Kbps for the electronics in the body domain.

CAN protocol uses a bitwise arbitration mechanism, called carrier sense multiple access with collision detection (CSMA/CD) for providing random access to the bus. The CAN protocol controls bus traffic by allowing high-priority messages access to the bus over lower-priority messages. Every message begins with the arbitration field, which identifies the message and determines its priority. If two or more nodes attempt to transmit messages at the same time, the node with the lowest numeric identifier wins the arbitration and continues with the transmission of its message. The other nodes will retire from contention and must wait until the bus becomes idle again before attempting to re-transmit their messages. The requirement of this mechanism is that the duration of each bit must be sufficient for the signal to propagate the length of the network.

Data frames are used for information transmission over CAN network. There are two different formats of CAN messages, according to the type of message identifier that is used by the protocol. Standard and extended frames are frames with 11-bit and 29-bit identifier fields, respectively. Each frame starts with a dominant synchronization bit, signaling to all receivers to synchronize their clocks. It is followed by an arbitration filed, which may be either 11 bits (CAN 2.0A) or 29 bits (CAN 2.0B). It is used to determine which node can access the bus and also to identify the type of data that message contains. The next field is the control field which specifies mainly the number of bytes of data contained in the message. The cyclic redundancy check (CRC) field is 15 bits long. The receiver uses the value in this field to detect the possible transmission errors in the data field. The acknowledgment (ACK) filed consists of two bits. The transmitter node expects from at least one receiver to acknowledge the error-free reception of the transmitted message. This acknowledgment is given by the transmission of a dominant bit in the acknowledge slot by all nodes in the network which received the message free of errors.

2.3 Related Work on Random Access MAC Protocols for V-PLC

When multiple users try to communicate with each other via shared transmission medium, there is a need for a MAC protocol to resolve the contention between users. MAC protocols for PLC networks can be grouped into two categories, namely, contention-free and contention-based MAC protocols. Contention-free protocols are mainly the ones based on time-division multiple access (TDMA), frequency-division multiple access (FDMA), or code-division multiple access (CDMA). Contention-free

MAC protocols usually rely on a central control point and perform very poorly when the number of contending nodes is unknown or keeps varying. On the other hand, contention-based MAC protocols are random access protocols, and usually operate in a distributed manner. They can be categorized into carrier sense multiple access-(CSMA-) based or non-CSMA-based MAC protocols. In this thesis, we focus on designing CSMA-based MAC protocols for V-PLC system.

Yamar Electronics Ltd. introduced a CSMA-based protocol for in-vehicle PLC, which is referred to as CDR protocol [1]. It uses several slots to resolve the contention among contending nodes. Each node randomly switches between carrier sense and carrier transmission modes. During a slot, when a node hears a carrier, it drops out of the contention, and the other nodes move to the next slot. This procedure repeats until the end of contention, and the goal of the protocol is to have only one survivor by the end of contention with a high probability.

The following steps are executed with respect to a single node:

1 . An n-bit register is constructed, whose content is randomly determined prior to each packet transmission.

2 . The node waits until the bus is idle, followed by a random time delay.

3 . The node switches between carrier sensing and carrier transmission according to the bit content of the register in step 1. The node performs carrier sensing if the bit content is zero and carrier transmission otherwise.

4 . The node proceed with the transmission of its preamble if no carrier was detected during any of the carrier sensing modes. Otherwise, if the carrier is detected, the node retires from contention.

We later present three alternative MAC protocols in Chapters 3-5. We show that our proposed MAC protocols perform considerably better than CDR in all scenarios.

2.4 Basics of Carrier Sensing and Impulse Filtering

Carrier sensing is a fundamental mechanism in CSMA-based MAC protocols. Each user senses the channel before a transmission and defers its transmission if it senses a busy channel to reduce the collision. There are typically two types of errors associated with the carrier sensing module: false alarm and miss detection probabilities. These probabilities are widely used as performance criteria for different sensing schemes. The probability of false alarm is the probability that the carrier is absent but is sensed as present by the user. The probability of missed detection is the probability that the carrier is present but is sensed as absent by the user. Comparisons between different carrier sensing schemes are usually done based on these two types of errors.

In carrier sensing, there are two hypotheses, where $\mathcal{H}_0$ is denoted as the hypothesis that a carrier is absent and $\mathcal{H}_1$ as the hypothesis that a carrier is present. The received signal for these hypotheses can be expressed as

$$\begin{aligned} \mathcal{H}_0 &: r(t) = n(t) \\ \mathcal{H}_1 &: r(t) = h\ s(t) + n(t) \end{aligned} \tag{2.1}$$

where $s(t)$ and $n(t)$ denote the transmitted signal and noise, respectively.

Energy detection is the most common detector in carrier sensing with a low cost

and hardware complexity. In energy detection, the received signal is squared and integrated within a bandwidth W over time period T, and is compared with a pre-defined threshold λ. If it exceeds the threshold (hypothesis $\mathcal{H}_1$), the detector declares the presence of the transmitted signal; otherwise, it is decided that there is no transmission in the sensed frequency channel (hypothesis $\mathcal{H}_0$). The time-bandwidth product is $u = TW$, and is assumed to be a positive integer.

The decision statistics of the energy detector is the average energy of the received signal and can be expressed as

$$T = \frac{1}{2u} \sum_{k=1}^{2u} |r(k)|^2 \tag{2.2}$$

where $r(k)$ denotes the received signal sampled at sampling frequency f_s, and $2u$ is the total number of samples taken from the received signal.

To determine whether the channel is busy, the detection statistics is compared with a predetermined threshold λ. The probability of false alarm p_f is the probability that the hypothesis test chooses $\mathcal{H}_1$ while it is in fact $\mathcal{H}_0$

$$p_f = P(T > \lambda | \mathcal{H}_0) \tag{2.3}$$

The probability of detection p_d is the probability that the test correctly decides $\mathcal{H}_1$ when it is $\mathcal{H}_1$

$$p_d = P(T > \lambda | \mathcal{H}_1) \tag{2.4}$$

We can also define the probability of miss detection as

$$p_m = 1 - p_d \tag{2.5}$$

Now assume the noise is a stationary AWGN. In this case, the probability of miss detection (p_m) and false alarm (p_f) can be calculated as [9]

$$p_m = 1 - Q_u(\sqrt{2\gamma}, \sqrt{\lambda}) \tag{2.6}$$

$$p_f = \frac{\Gamma(u, \frac{\lambda}{2})}{\Gamma(u)} \tag{2.7}$$

where $Q_u(.,.)$ is the generalized Marcum-Q function, $\Gamma(.,.)$ is the upper incomplete gamma function [10], and γ is the ratio of signal energy to one-sided noise spectral density, i.e., $\gamma = u \times \text{SNR}$, where SNR is the signal-to-noise ratio of the preprocessed signal.

The fact is that noise in power lines is not AWGN. Therefore, we can express the noise as

$$n(t) = w(t) + i(t) \tag{2.8}$$

where $w(t)$ and $i(t)$ denote the background Gaussian noise and impulsive noise component, respectively. Since the statistical behavior of the noise over V-PLC is unknown, it is best to remove the impulse components from the noise by using a robust impulse filtering technique. The overall structure of the detector is depicted in Fig. 2.1. The received signal passes through a band-pass filter (BPF) of bandwidth W and an Analog-to-Digital Converter (ADC) with sampling rate f_s to discretize the input signal, followed by a preprocessor and a linear signal detector. We use energy detector as a signal detection scheme for its low complexity. We would like to remark, however that any other signal detection scheme of interest can also be used in the system. We used the preprocessor proposed in [11] as it provides a simple real-time technique to replace the impulse components in the received signal. The preprocessor has an

impulse detector which is composed of a blanking nonlinearity to mitigate the effects of the impulsive corruptions, followed by a reconstruction filter that selects between input and predicted samples.

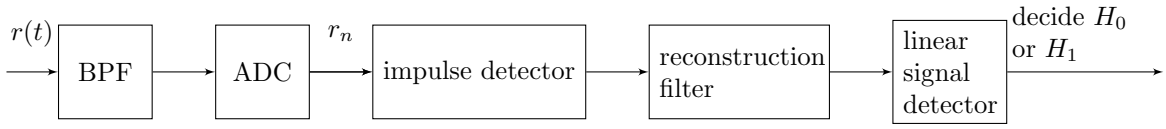

Figure 2.1: Block diagram of a robust signal detector.

We performed an experiment to illustrate the effectiveness of the preprocessor. Consider the received signal is corrupted by a Gaussian noise with variance one, plus an impulsive noise with probability of occurrence 0.1 and variance 10. Fig. 2.2 shows one thousand samples of the received signal before and after preprocessing. It can be observed that the preprocessor successfully removes the impulses from the signal. To better understand its performance, we plotted the empirical cumulative distribution function (ECDF) of the received signal in Fig. 2.3. It can be seen that the preprocessor removes the heavy tail of the signal, and the preprocessed signal almost matches the Gaussian distribution, i.e., impulse-free signal. We then use an energy detector which compares the average energy of the output of the preprocessor over the sensing period T to a predetermined threshold λ. The time-bandwidth product is $u = TW$, and is assumed to be a positive integer. The probability of miss detection (p_m) and false alarm (p_f) can be calculated as in (2.6) and (2.7).

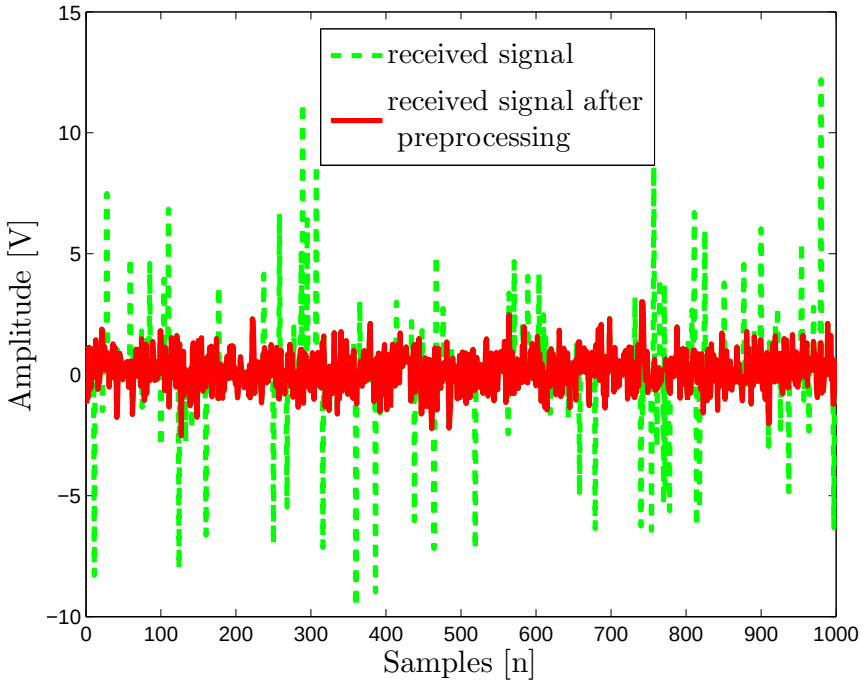

Figure 2.2: Samples of the received signal before and after preprocessing.

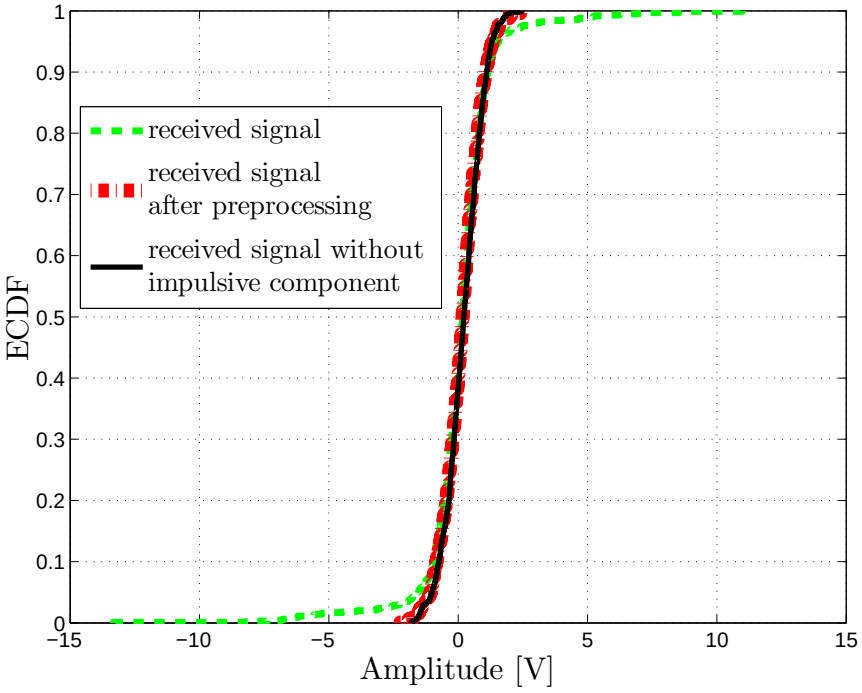

Figure 2.3: ECDF of the real, preprocessed, and impulse-free received signal.

Chapter 3

Frequency-Domain Contention Resolution Algorithm with Imperfect Carrier Sensing

In this chapter, we present a MAC protocol for V-PLC system, which uses a combination of time and frequency multiplexing to resolve the contention among nodes. We first present our motivations and assumptions, followed by system model. We find the optimal parameters of the protocol with the assumption of imperfect carrier sensing in Section 3.3. In Section 3.4, we present the performance evaluation of the proposed scheme using numerical examples, followed by a summary of the chapter in Section 3.5.

3.1 Motivations and Assumptions

Yamar Electronics Ltd. introduced a contention-based MAC protocol for V-PLC system, referred to as CDR, in [1]. The protocol uses several slots to arbitrate packet transmission. It resolves the contention between contending nodes by switching between carrier transmission and carrier sensing modes in each slot. Similar to CDR protocol, our proposed MAC scheme tries to arbitrate packet transmission over power lines. Our protocol, however, uses multiple frequency channels to arbitrate packets

within slots. Hence, it is a novel solution to overcome the frequency-selective behavior of V-PLC transmission channels. CDR does a good job in handling scenarios with small numbers of nodes, but does not handle large numbers of nodes well. The authors in [12] designed a MAC protocol called Alert for low latency applications. It attempts to resolve a contention through randomized subcarrier assignments that are optimized to minimize latency. Our protocol is similar to Alert in the sense that it uses the same subcarrier/round structure. However, our approach does not require that the sum of the subcarrier selection probabilities be equal to unity; in other words, nodes may or may not choose a subcarrier. We show later, that this approach improves the MAC layer performance. Moreover, we generalize the solution proposed in [12] by examining the effects of carrier sensing errors on the MAC layer efficiency. We also construct a cross-layer optimization problem, and obtain the optimized physical layer (PHY) and MAC layer parameters together.

3.2 System Model

We assume the system uses a multi-carrier physical layer as proposed in [8]. Our scheme follows the model depicted as in Fig. 3.1. The channel is assumed to be idle when nodes simultaneously try to transmit packets. Data transmission is divided into contention rounds and multiple subcarriers are available in each round. We present our protocol concepts with an example. Assume two nodes N_1 and N_2 are trying to transmit a packet to node R. Each node, with a probability that we define, starts with the transmission of its preamble on the subcarrier index i, chosen from $1, \ldots, N_c$. Further assume that, each node is equipped with a single transceiver; thus, can not simultaneously transmit and receive packets. Here, assume N_1 and N_2 have transmitted on subcarriers f_1 and f_2, respectively, and $f_1 < f_2$. At the beginning of

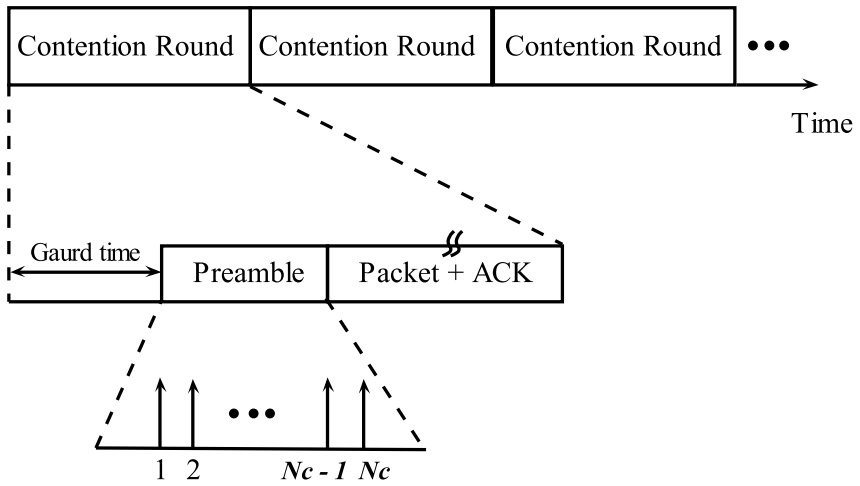

Figure 3.1: A view of the frame structure.

the contention round, R listens for signals on all subcarriers starting from subcarrier index 1, and if any are detected, it locks on the subcarrier and waits to receive the packet. In this example, since N_1 has transmitted on the earlier subcarrier, it wins the contention. If the packet is received correctly, R sends back an ACK over subcarrier f_1 at the end of the contention round. There are, however, some scenarios that might cause R not to receive the packet sent by N_1. If R senses a high signal at subcarrier index $< f_1$, due to the interference or noise, R never receives a packet from any node. If R does not detect the signal on subcarrier f_1, no packet arrives from N_1. It is obvious that theses sensing errors have a huge influence on the performance of the protocol.

There are two design parameters that need to be known while protocol is in operation. (1). number of subcarriers (2). probability distribution over subcarriers. We can reduce the contention between nodes by using a large number of subcarriers. However, this also results in larger time slots and reduces the number of time slots within a period, and therefore introduces a tradeoff. Similarly, assigning low probabilities to the low-indexed subcarriers while the workload is high would arbitrate the

packets. On the other hand, when the workload is low, assigning low probabilities to low-indexed subcarriers will result in longer delays. Therefore, it is important to find the values for these parameters which optimize the performance of the protocol.

3.2.1 Sensing Model

We follow the procedure described in Chapter 2 for carrier sensing. This means the received signal is passed through the preprocessor to remove the impulsive components. We then employ the commonly used energy detector for channel sensing due to its simplicity. We should remark, however that, the analysis presented in this chapter can be easily extended for any other detection schemes as will be addressed in Section 3.3. Suppose that the received signal has passed through the preprocessor and is sampled at sampling frequency f_s. We are interested in detecting of the transmitted signal in a given subcarrier. In energy detection, the received signal is squared and integrated within a bandwidth W over time period T, and is compared with a pre-defined threshold η. If it exceeds the threshold (hypothesis $\mathcal{H}_1$), the detector declares the presence of the transmitted signal; otherwise, it is decided that there is no transmission in the sensed subcarrier (hypothesis $\mathcal{H}_0$). The received signal under two hypotheses at time t can be represented as

$$\begin{aligned} \mathcal{H}_0 &: r(t) = b(t) \\ \mathcal{H}_1 &: r(t) = hs(t) + b(t) \end{aligned} \tag{3.1}$$

where $b(t)$ is the noise signal at the receiver, and is assumed to be a circularly symmetric complex Gaussian (CSCG) random variable, independent and identically distributed (i.i.d.) with mean zero and variance σ_b^2. The samples of transmitted signal,

$s(t)$, also follows CSCG, i.i.d. sequence with mean zero and variance σ_s^2, and the PLC channel gain h is set to unity. In energy detection, the probabilities of false alarm (p_f) and miss-detection (p_m) can be evaluated by [10]

$$p_f = p\left(\text{decide } \mathcal{H}_1 \mid \mathcal{H}_0\right) = 1 - \Gamma(N_s, \frac{\eta}{\sigma_b^2}) \tag{3.2}$$

$$p_m = p\left(\text{decide } \mathcal{H}_0 \mid \mathcal{H}_1\right) = \Gamma(N_s, \frac{\eta}{\sigma_b^2 + \sigma_s^2}) \tag{3.3}$$

where N_s denotes the number of samples taken by the receiver at each subcarrier. $\Gamma(x,t) = \frac{\int_0^t e^{-y} y^{x-1} \mathrm{d}y}{\int_0^\infty e^{-y} y^{x-1} \mathrm{d}y}$ is the incomplete gamma function. The detection threshold is given by [10]

$$\eta = \sigma_b^2 \Gamma^{-1}(N_s, 1 - p_f) \tag{3.4}$$

$\Gamma^{-1}(x;.)$ is the inverse function of $\Gamma(x;.)$ with respect to its second variable. Finally, we can express p_m in terms of p_f as

$$p_m = \Gamma\left(N_s, \frac{1}{1+\gamma}\Gamma^{-1}(N_s, 1 - p_f)\right) \tag{3.5}$$

where signal–to–noise ratio (SNR) at the receiver is denoted as $\gamma = \frac{\sigma_s^2}{\sigma_b^2}$. We assume SNRs are different at each subcarrier, and can be expressed as γ_i for $i = 1, 2, \ldots, N_c$. Therefore, in the remainder of the chapter, p_m^i and p_f^i correspond to the probability of miss-detection and false alarm of the subcarrier index i, respectively.

3.2.2 Probability of Successful Transmission

The channel is assumed to be idle when nodes try to send data onto the medium at the same time. Each node may choose one of N_c subcarriers to send its data. Let $p = (p_1, p_2, \ldots, p_{N_c})$ be the *selection distribution* that each node uses to select one of

N_c subcarriers. We say that subcarrier j is successful *if and only if*

(i) j is the smallest index among chosen subcarriers and there is no false alarm error on the earlier subcarriers.

(ii) there is only one node transmitting on the subcarrier j with no miss-detection error.

Suppose that number of nodes in a contention is n. The probability of successful transmission is

$$p_s^n = n \sum_{j=1}^{N_c} p_j (1-p_j)^{n-1} (1-p_m^j) \prod_{t=0}^{j-1} (1-p_t)^n (1-p_f^t) \tag{3.6}$$

where $p_f^0 \triangleq 0$ and $p_0 \triangleq 0$.

Let S_1 be a random variable that shows the number of rounds required to successfully receive the first packet from n nodes. If the probability of success in each round is constant and equal to p_s^n, then the probability that m^{th} round is the first success has a Geometric distribution with expected value $\frac{1}{p_s^n}$ ($S_1 \sim \text{Geom}(p_s^n)$), and is defined as

$$\mathbf{P}(S_1 = m) = p_s^n (1-p_s^n)^{m-1} \quad m = 1, 2, \ldots \tag{3.7}$$

where we assumed that the PHY parameters are constant in each round which leads to a constant probability of success. By the same argument, we need $\text{Geom}(p_s^{n-1})$ rounds to receive the second packet. In general, the distribution of the number of rounds required to receive the k^{th} packet successfully is

$$S_k \sim \sum_{i=n-k+1}^{n} \text{Geom}(p_s^i) \tag{3.8}$$

3.2.3 Time Utilization

From our previous discussions, it is clear that we can reduce the expected number of rounds to receive packets by using a larger number of subcarriers in a contention round. On the other hand, a larger number of subcarriers increases the length of a contention round. We define the average time utilization corresponding to the first k received packets ρ_k as

$$\rho_k = \frac{k(t_d + t_{ack})}{\mathbf{E}(S_k)T_{CR}} \tag{3.9}$$

where t_d and t_{ack} are time durations required for data and acknowledgment transmissions, respectively. $\mathbf{E}(S_k)$ is the expected value of number of contention rounds to successfully receive k packets, and the duration of a contention round T_{CR} is

$$T_{CR} = \frac{N_s}{f_s} N_c + t_d + t_{ack} \tag{3.10}$$

where $\frac{N_s}{f_s}$ specifies the sampling time required by the receiver to take N_s samples from a subcarrier. Note that in (3.10), we assumed that the switching time between subcarriers is negligible.

3.3 Optimal Selection Distribution

In this section, we find the selection distribution p^* and sensing threshold η^* that maximizes p_s^n, the probability of successful packet delivery in one round for a known number of nodes. We derive optimal distributions in the cases of both finite and

infinite number of nodes.

3.3.1 Analysis of Optimal Scheme with Finite n

First, we assume that the values of p_m and p_f for each subcarrier are known. Then, the question is what is the selection distribution that maximizes the probability of successful transmission for known sensing errors?

Proposition 1: For a given p_m^i and p_f^i, $i = 1, \ldots, N_c$, the probability distribution that maximizes (3.6) satisfies the following recursive equation

$$p_k^* = \frac{1 - (1 - p_{k+1}^*)^{n-1} v_k (1 - p_m^{k+1})}{n - (1 - p_{k+1}^*)^{n-1} v_k (1 - p_m^{k+1})} \tag{3.11}$$

for $k = 1, \ldots, N_c - 1$ with $p_{N_c}^* = \frac{1}{n}$, and

$$v_k = \frac{1 - p_f^k}{1 - p_m^k} \tag{3.12}$$

Proof: Assume that the values of p_i^*, $i = 1, 2, \ldots, N_c - 1$ are already known. Then, $p_{N_c}^*$ maximizes (3.6) if $\frac{d}{dp_{N_c}^*}(p_s^n) = 0$. Differentiating (3.6), we have $\left(1 - p_{N_c}^*\right)^{n-1} - (n-1)p_{N_c}^* \left(1 - p_{N_c}^*\right)^{n-2} = 0$. One solution is $p_{N_c}^* = 1$ which is clearly not the optimal answer, and the second solution is $p_{N_c}^* = \frac{1}{n}$. Next, by a similar approach, we derive $p_{N_c-1}^*$ assuming that the values of p_i^*, $i = 1, 2, \ldots, N_c - 2$ are known. Again, one solution is $p_{N_c-1}^* = 1$, and the acceptable answer is the one given in (3.11), with $k = N_c - 1$. Repeating this procedure yields to the optimum distribution in (3.11).

After obtaining the optimum selection distribution p^* in terms of carrier sensing errors, we range p_f^i, $i = 1, \ldots, N_c$ in (3.5) from 0 to 1 for a given N_s and SNR, and obtain p_f and p_m for each subcarrier which are optimized to maximize the probability of successful transmission in (3.6). The following example is given to further illustrate

the design procedure.

Example 1: Consider a V-PLC network with $n = 5$ nodes and $N_c = 10$ subcarriers. The energy detector takes $N_s = 10$ samples from a transmitted signal in each subcarrier. We consider the following two cases:

1 . all subcarriers have the same SNR and is equal to 0dB.

2 . subcarrires have different SNRs and the relation is given by

$$\gamma_k = \gamma_m + 10(k-1)\log\alpha; \qquad k = 1, 2, \ldots, N_c$$

where k is the subcarrier index, $\gamma_m = 5$dB, and $\alpha = 0.8$. Using the results in proposition 1, we can obtain the optimal parameters (p^*, p_f^*, p_m^*) as shown in Table 3.1. The results, in both cases, show that the subcarrier selection probability p_k^* increases as k increases. The probability of success for case 1 and 2 are 0.577 and 0.7496, respectively. We also would like to note that using (3.4), we can determine the optimum detection threshold η_k^* for a given noise variance in each subcarrier.

For this example with no sensing errors, our scheme and Alert [12] achieve the probability of success of 0.8668 and 0.8541, respectively. As previously mentioned, in our model, the sum of subcarrier selection probabilities may not be equal to 1, and thus provides more chance for nodes to choose different subcarriers which leads to a higher probability of success.

3.3.2 Asymptotic Analysis of Optimal Scheme as $n \to \infty$

We now provide asymptotic expressions for optimum selection distribution and maximum probability of success when $n \to \infty$.

Table 3.1: Optimal Parameters in Example 1

	Case 1			Case 2		
	p^*	p_f^*	p_m^*	p^*	p_f^*	p_m^*
k						
1	0.0813	0.0921	0.1899	0.064	0.0058	0.0234
2	0.0819	0.0929	0.1888	0.0715	0.0125	0.0399
3	0.0828	0.0943	0.1871	0.0797	0.0249	0.0621
4	0.0843	0.0963	0.1846	0.0888	0.0463	0.0879
5	0.0868	0.0998	0.1803	0.099	0.0804	0.1144
6	0.0912	0.1065	0.1776	0.1109	0.1325	0.1362
7	0.0987	0.1187	0.16	0.1262	0.2146	0.1444
8	0.1118	0.1416	0.14	0.1474	0.3478	0.129
9	0.1372	0.2016	0.1021	0.1985	0.977	0.0014
10	0.2	1	$\simeq 0$	0.2	1	$\simeq 0$

Proposition 2: The maximum probability of successful transmission for $n \to \infty$ is given by

$$p_s^{\infty} = (1 - p_m^1)e^{-q_1^*} \tag{3.13}$$

where q_k^* for $k = 1, 2, \ldots, N_c$ is recursively defined as

$$q_k^* = \begin{cases} 1 & \text{for } k = N_c \\ 1 - \frac{(1-p_f^k)(1-p_m^{k+1})}{(1-p_m^k)} e^{-q_{k+1}^*} & \text{else.} \end{cases}$$

Proof: As discussed earlier, the selection probabilities depend on number of nodes. Therefore, in order to get a non-zero probability of success, we assume that the optimal probabilities are expressed as $p_k^* = \frac{q_k^*}{n}$ for $k = 1, 2, \ldots, N_c$. By using these probabilities in (3.6) and taking $n \to \infty$, we have

$$p_s^{\infty} = \sum_{j=1}^{N_c} q_j^* e^{-q_j^*} (1 - p_m^j) \prod_{t=0}^{j-1} e^{-q_t^*} (1 - p_f^t) \tag{3.14}$$

where we used $\lim_{n\to\infty}(1+\frac{x}{n})^n = e^x$ for $x \in \mathbf{R}$. Taking the derivation of (3.14) with respect to q_i^* $i = 1, \ldots, N_c$, and imposing it equal to zero, we obtain

$$e^{-q_i^*}(1-p_m^i)\prod_{t=0}^{i-1} e^{-q_t^*}(1-p_f^t)\left(1-\sum_{j=i}^{N_c} q_j^* \right. \\ \left. e^{-\sum_{k=i+1}^{j} q_k^*}\frac{1-p_m^j}{1-p_m^i}\prod_{t=i}^{j-1}(1-p_f^t)\right) = 0 \tag{3.15}$$

hence,

$$\sum_{j=i}^{N_c} q_j^* e^{-\sum_{k=i+1}^{j} q_k^*}\frac{1-p_m^j}{1-p_m^i}\prod_{t=i}^{j-1}(1-p_f^t) = 1 \tag{3.16}$$

Setting $i = N_c$ in (3.16) gives $q_{N_c}^* = 1$. Then, for $i = 1, 2, \ldots, N_c - 1$, we can rewrite (3.16) as

$$1 = q_i^* + \frac{(1-p_f^i)(1-p_m^{i+1})e^{-q_{i+1}^*}}{1-p_m^i} \\ \sum_{j=i+1}^{N_c} q_j^* e^{-\sum_{k=i+2}^{j} q_k^*}\frac{1-p_m^j}{1-p_m^{i+1}}\prod_{t=i+1}^{j-1}(1-p_f^t) \tag{3.17}$$

It can be seen that the summation in (3.17) is the same as (3.16) for $i+1$, and therefore is equal to one which gives the solution in (3.13). As an example, with no sensing errors, we can achieve the probability of success of 0.8418 with $N_c = 10$ subcarriers which is very close to the one previously calculated in example 1 for $n = 5$ nodes.

3.4 Numerical Results

In this section, we present some numerical results to evaluate the proposed MAC scheme with different PHY parameters. PHY bit rate is 1Mbps, and the payload size

of a packet is fixed to 64 Bytes [14]. Transmitted signal is sampled at a frequency of 100MHz to avoid aliasing errors [6]. Throughout this section, we assume, for simplicity, that all subcarriers have the same SNR.

3.4.1 Performance under Different SNRs

In this experiment, number of nodes is fixed at 16. The channel average SNR varies from -15dB to 15dB. The probability of successful transmission for different number of subcarriers at $N_s = 10$, and for different number of samples at $N_c = 8$ are shown in Fig. 3.2 and Fig. 3.3, respectively. It can be seen that, given the same number of

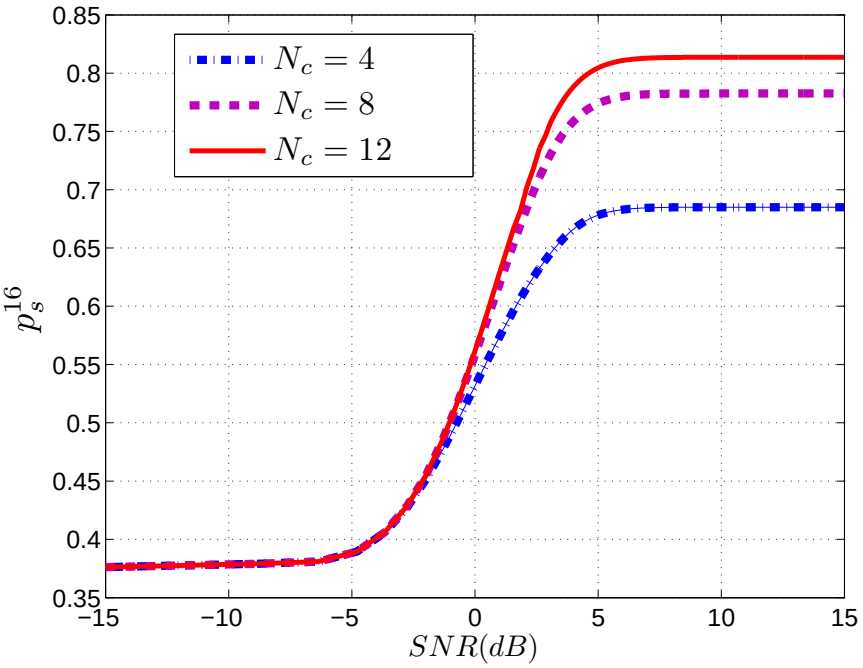

Figure 3.2: Probability of successful transmission versus SNR for different number of subcarriers at $N_s = 10$.

sampling, p_s increases as SNR increases. Note also that a higher N_c leads to a larger value for p_s. This is expected as increasing the number of subcarriers increases the likelihood that nodes select different subcarriers and thus yields higher p_s. As shown

in Fig. 3.3, by increasing N_s, we can achieve the same p_s for smaller values of SNR. However, the difference tends to dwindle in the high SNR region (SNR≥5dB).

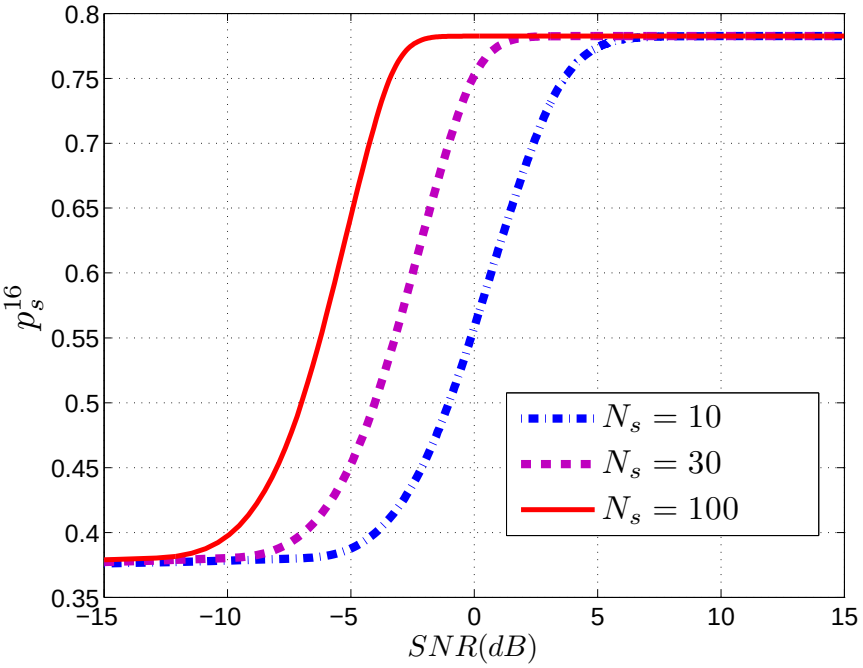

Figure 3.3: Probability of successful transmission versus SNR for different number of samples at $N_c = 8$.

3.4.2 Performance under Different Number of Nodes

The effect of number of nodes on the probability of success for multiple cases is illustrated in Fig. 3.4. N_c is 8, and N_s is set to 10. For a fixed SNR, as n increases, p_s^n drops initially, then becomes almost constant. It can be observed that with perfect sensing, we can achieve highest p_s^n, and the probability of success drops as SNR decreases.

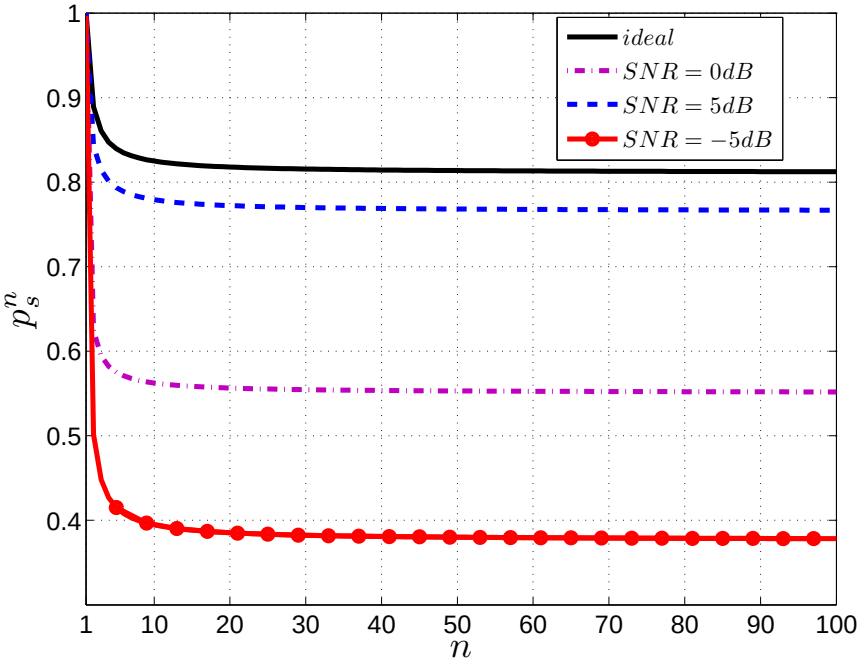

Figure 3.4: Probability of successful transmission as a function of number of nodes for different SNRs, $N_c = 8$ and $N_s = 10$.

3.4.3 Time Utilization

Number of nodes in a contention is 16 and the channel SNR is set to -5dB. Fig. 3.5 shows time utilization of the first packet as a function of N_s and N_c for the proposed design approach. For a fixed number of subcarriers, ρ_1 increases with number of sampling and then decreases. This happens since increasing N_s leads to a lower $\mathbf{E}(S_1)$ as shown in Fig. 3.3. On the other hand, as we increase N_s, the length of each round is increased, and therefore there is a value for N_c that maximizes ρ_1. Similarly, for a fixed number of sampling, ρ_1 increases with number of subcarriers and then decreases. Furthermore, we notice from Fig. 3.5 that the maximum time utilization is 0.76, and is occurred at $N_c = 13$ and $N_s = 261$.

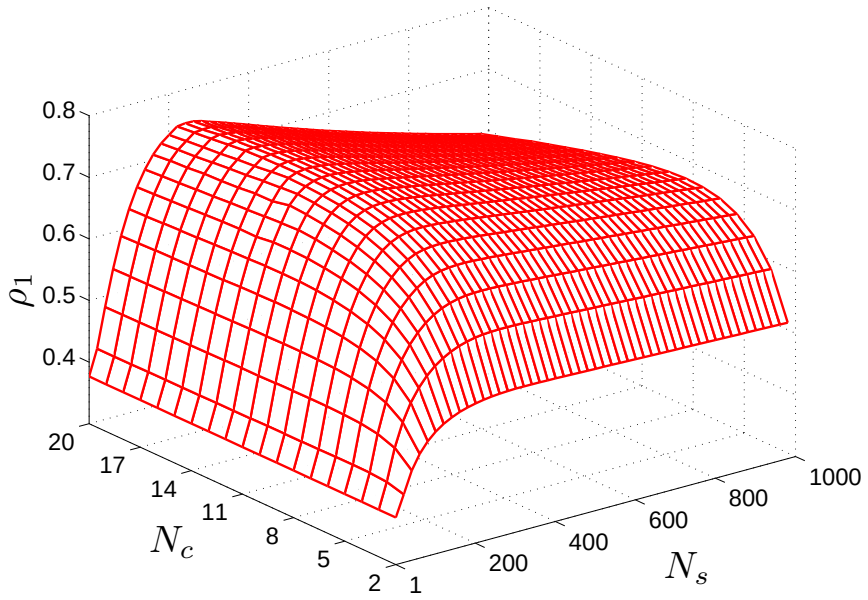

Figure 3.5: ρ_1 versus N_s and N_c, SNR = -5dB and $n = 16$.

3.4.4 Comparison with CDR Protocol

In this subsection, we compare the performance of the proposed scheme with CDR [1]. We plot the probability of success for different values of N_c for both protocols as shown in Fig. 3.6. To make a fair comparison, we note that using N_c subcarriers in our scheme increases the packet overhead by the same length as employing N_c slots in the ER of CDR protocol. Number of contending nodes varies from 2 to 100. The results show that the success rates of both schemes decrease as the network size grows. However, the decrease rate of our scheme is much lower than that of CDR. CDR is observed to have a slightly better performance when the number of contending nodes is small. However, our scheme outperforms CDR when network size increases, and disparity between two schemes becomes larger as number of nodes increases.

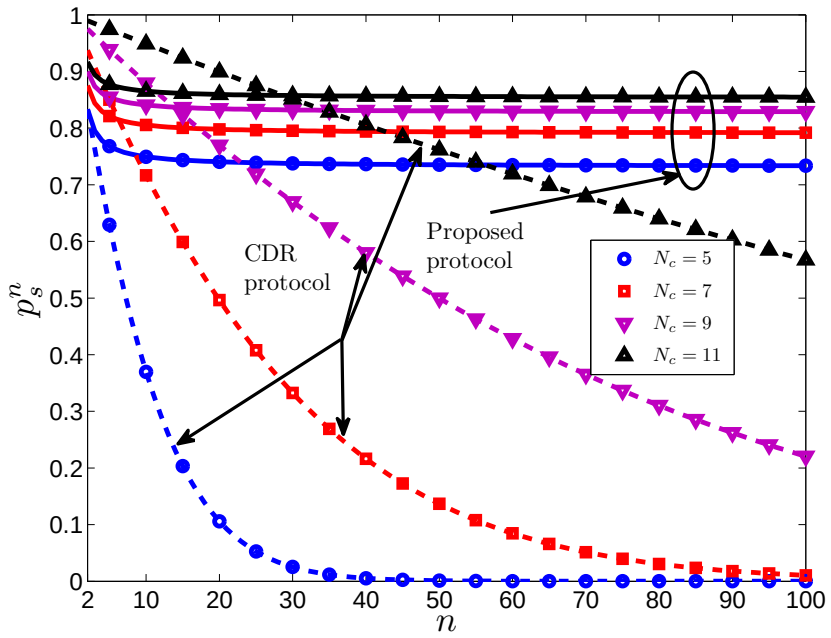

Figure 3.6: Probability of successful transmission of the proposed and CDR protocol as a function of number of nodes.

3.5 Summary

In this chapter, we have introduced a random access MAC protocol which uses a novel contention mechanism in which nodes use subcarriers to perform channel contention. Through mathematical analysis, we have examined the effect of carrier sensing errors on the protocol performance. We have derived expressions for optimum selection distribution p^* that nodes employ to choose a subcarrier for data transmission, and for design parameters involved in carrier sensing scheme. With numerical examples, we have verified the effectiveness of our proposed scheme.

Chapter 4

Time-Domain Contention Resolution Algorithm with Imperfect Carrier Sensing

In the previous chapter, we introduced a MAC protocol that resolves the contention between nodes by using multiple frequency channels. Now, we focus on MAC protocols which attempt to resolve the contention on a given frequency channel in a constant number of slots. We first state our motivations and assumptions. We then describe the system model and give an example of the protocol operation in Section 4.2. Section 4.3 presents the detailed analysis of the protocol under carrier sensing failures. Section 4.4 provides numerical examples and finally summary is given in Section 4.5.

4.1 Motivations and Assumptions

In Chapter 2, we described the previously developed contention-based MAC protocol, referred to as CDR, for V-PLC system in detail. Here, we briefly state its operation. CDR resolves the contention in a number of slots by randomly switching between carrier sense and carrier transmission modes. During a slot, nodes drop out of contention, if they were listening and hear a carrier on the bus. The remaining nodes

survive and move to the next slot. This process repeats until the contention finishes and the goal here is to have one survivor at the end of the contention with a high probability. The authors in [1] provided mathematical analysis of the protocol with the assumption of perfect carrier sensing.

However, as mentioned in Chapter 2, the measurements of V-PLC channels [4, 7], show that it is necessary to analyze the performance of the MAC protocols under carrier sensing errors to improve the overall system performance. Hence, the objective of this chapter is to extend the study of contention based MAC protocols suitable for in-vehicle PLC to the more realistic scenario of imperfect carrier sensing. To this end, we consider the MAC protocol from [13], which is called *selective tournaments*, and is very similar to CDR. In particular, as in CDR, it switches between carrier sense and carrier transmission in each slot. However, nodes use a unique nonuniform probability distribution to select their operation in each slot, which minimizes the collision between contending nodes, and hence offers a fast contention resolution while its performance degrades at a much slower rate than CDR with the increase in number of contending nodes.

4.2 System Model

We consider a network setting where n_c nodes are connected to the harness. We assume time is slotted and nodes in the network are time synchronized. We further assume that each node in the network is equipped with a half-duplex transceiver, i.e., it cannot transmit and listen to one channel at the same time. Nodes with packets to transmit contend over a fixed number of slots. Nodes choose to transmit a carrier on the bus by using a probabilistic approach. In a given slot, nodes lose the contention if they were sensing the bus and hear a valid carrier. Otherwise, they move

to the next slot. We use the procedure described in Chapter 2 for carrier sensing, where sensing is performed by preprocessing the received signal so that it contains no impulsive component and then applying energy detection on the preprocessed signal. The protocol operation under imperfect carrier sensing will be presented in the next subsection. The mathematical formulation of the protocol, as well as the analysis of the carrier sensing error on the performance of the protocol are presented in Section 4.3. We then present the numerical results to evaluate the performance of the protocol under imperfect carrier sensing, followed by a summary of the chapter in Sections 4.4 and 4.5, respectively.

4.2.1 MAC Protocol Operation

We now describe the operation of the selective tournaments MAC protocol in detail. We also show that, by considering different scenarios, how carrier sensing errors can affect the results of the operation. The protocol resolves the contention between contending nodes over n_s slots. All the contending nodes go through the following procedure. Before the i^{th} slot with $i \in \{1, 2, \ldots, n_s\}$, a node generates a binary random integer c_i with a predetermined probability. It then transmits a carrier on the bus if $c_i = 1$. Otherwise, it listens to the bus for a slot duration. We denote $c_i = 0$ and 1 as *signal 0* and *signal 1*, respectively. A node that is listening and senses the bus busy will retire from the contention. On the other hand, if a node senses the bus idle, it stays in the contention. A node that transmits a carrier on the bus survives and moves to the next slot.

Fig. 4.1 illustrates an example of the protocol with three slots. The left and right branches correspond to the events of choosing signal 1 and 0, respectively. Assume nodes A and B have packets to transmit. In the first slot, each node chooses signal 1

with probability q. In this example, both nodes selected signal 0, and moved to the second slot. Now assume node A has detected a carrier due to the false alarm. In that case, node A would retire from contention. In the second slot, a node chooses signal 1 with probability q_1 if it has emitted a carrier in the first slot, and with probability q_0 otherwise. Here, in the second slot, nodes A and B have selected signal 1 and 0, respectively. Thus, node A preempts node B. However, in this example, we have assumed that node B has not detected the carrier from node A, and hence stayed in the contention (miss detection error). In the third slot, both nodes chose to transmit a carrier, and therefore survived the whole process. We can describe the whole process with a set of three binary digits. We can then conclude that a node with the largest value wins the contention. However, this might not be true with the presence of sensing errors. In this example, nodes A and B have chosen 011 and 001, respectively. Hence, node A has a larger binary value and wins the contention with the assumption of perfect carrier sensing. However, the result is unknown with imperfect sensing as in the above example, both nodes won the contention.

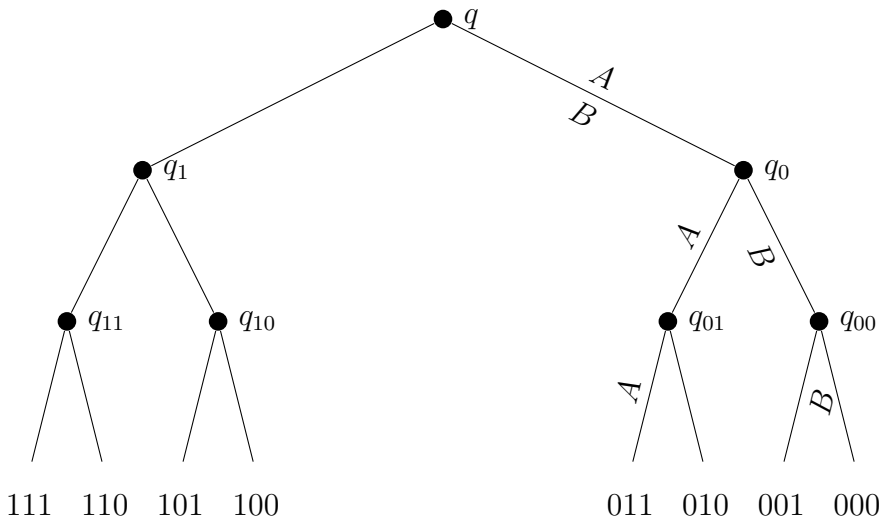

Figure 4.1: Illustration of the protocol operation.

4.3 MAC Protocol Analysis

This section presents an analysis to provide an insight into the impact of imperfect carrier sensing on the performance of selective tournaments MAC protocol.

We consider a PLC network with a total population of n_c nodes. We model the number of contending nodes at a given time by a truncated power-law degree distribution due to its flexibility, which is given by

$$p_{n_c,n} = \frac{1}{\zeta(\gamma) n^{\gamma}} \tag{4.1}$$

with $n \in \{2, \ldots, n_c\}$, and $\zeta(\gamma) = \sum_{z=2}^{n_c} \frac{1}{z^{\gamma}}$ is the scaling factor to make the probabilities sum to one. This distribution is widely applied to model self-similar arrival in packet traffic. However, we would like to point it out that the analyses in this chapter are valid for any other distribution of interest.

4.3.1 Probability Distribution of Survivors

We define $G(z)$ as the probability generating function for the number of contending nodes, which is given by

$$G(z) := \mathbf{E}(z^n) = \sum_{n=2}^{n_c} p_{n_c,n}\ z^n \tag{4.2}$$

We derive the probability generating function for the number of contending nodes still in the contention after the elapse of one time slot. We know that if a node that is listening does not hear the carrier on the bus, it will select itself as a winner. So, depending on the number of nodes who choose signal 1, we derive expressions for the distribution of survivors. We use subscripts 0 and 1 on probability generating

functions to denote the cases when all nodes choose signal 0 or at least one node chooses signal 1, respectively. We first calculate the probability generating function for the case when all nodes choose to listen to the bus, which can be expressed as

$$\begin{aligned} G_0(z) &= \sum_{n=2}^{n_c} p_{n_c,n}(1-q)^n \sum_{i=0}^{n} \binom{n}{i} (1-p_f)^i p_f^{n-i} z^i \\ &= \sum_{n=2}^{n_c} p_{n_c,n}(1-q)^n \left[(1-p_f)z + p_f\right]^n \\ &= G\left((1-q)z_f\right) \end{aligned} \tag{4.3}$$

where $z_f := (1-p_f)z + p_f$. q is the probability of transmitting a carrier in the first slot, and p_f is the false alarm probability given in (2.7). In this case, a node moves to the second slot if it has not detected a carrier on the bus, which happens with probability $1-p_f$. We used Binomial distribution to denote the probability that i out of n nodes have not detected the carrier, and thus moved to the second slot.

We now derive the probability generating function for the number of surviving nodes conditioning that at least one node has transmitted a carrier in the first slot. The expression for G_1 is given by

$$\begin{aligned} G_1(z) =& \sum_{n=2}^{n_c} p_{n_c,n} \sum_{i=1}^{n} \binom{n}{i} q^i (1-q)^{n-i} z^i \\ & \sum_{j=0}^{n-i} \binom{n-i}{j} p_m^j (1-p_m)^{n-i-j}\ z^j \\ &= G\left(qz + (1-q)z_m\right) - G\left((1-q)z_m\right) \end{aligned} \tag{4.4}$$

where $z_m := p_m z + 1 - p_m$, and p_m is the miss detection probability defined in (2.6). In this case, all nodes that have transmitted a carrier in the first slot survive and move to the second slot. However, nodes that chose to listen to the bus and have detected

the carrier, which happens with probability $1 - p_m$ would retire from contention. Others that have listened to the bus and did not hear the carrier (with probability p_m) will continue the contention.

We denote $c = [c_1 \dots c_i \dots c_k]$ as the *signaling pattern* of a node in the first k slots, i.e., $c_i = 1$ and 0 correspond to signal 1 and 0, respectively. We are now interested in calculating the probability generating function of survivors after the elapse of $k + 1$ slots. By mathematical induction and using (5.13) and (5.14), we have

$$G_{c0}(z) = G_c\left((1 - q_c)z_f\right) \tag{4.5}$$

and

$$G_{c1}(z) = G_c\left(q_c z + (1 - q_c)z_m\right) - G_c\left((1 - q_c)z_m\right) \tag{4.6}$$

where q_c is the probability of emitting a carrier in slot $k + 1$, given the signaling pattern c in the first k slots. G_c is the probability generating function of survivors corresponding to the signaling pattern c, and $G_\varnothing := G$. Hence, the probability generating function of survivors after n_s slots is $\sum_{c\in\mathcal{C}_{n_s}} G_c(z)$, where $\mathcal{C}_{n_s}$ contains all the codewords of length n_s form the alphabet $\{0, 1\}$. Moreover, the distribution of survivors is completely characterized by $p^{n_s}_{n_c,n} = \frac{1}{n!}\frac{d^n}{dz^n}\sum_{c\in\mathcal{C}_{n_s}} G_c(z)|_{z=0}$, where n is the number of winners at the end of the contention. We can compute the probability of successful transmission, which is defined as the probability that at the end of the contention only one survivor remains, by the following equation

$$p_s = p^{n_s}_{n_c,1} = \frac{d}{dz}\sum_{c\in\mathcal{C}_{n_s}} G_c(z)|_{z=0} \tag{4.7}$$

The system may remain idle even after the completion of contention. This can happen since there might be a situation where in a slot, all nodes in the contention

choose to listen and all of them hear a carrier due to the false alarm error, and hence retire from contention. This probability can be calculated as

$$p_i = p_{n_c,0}^{n_s} = \sum_{c \in \mathcal{C}_{n_s}} G_c(0) \tag{4.8}$$

and the probability that two or more nodes remain at the end of the contention, i.e., collision probability, is simply given by

$$p_c = 1 - p_s - p_i \tag{4.9}$$

We need to find the values for probabilities that nodes use to select between signal 1 and 0 in different slots, i.e., $\sum_{i=0}^{n_s-1} 2^i = 2^{n_s-1}$ parameters. We obtain these values by using the procedure provided in [13], which first approximates the collision rate with a Riemann integral and then obtains the parameters that minimizes the collision between nodes with the assumption of perfect carrier sensing. The proposed procedure is summarized in Algorithm 1, and optimal parameters for (n_c, n_s, γ)=(16, 6, 0.6) are presented in Table 4.1.

Suppose we use the optimum probabilities obtained from Algorithm 1 for a known $p_{n_c,n}$ with the assumption of perfect carrier sensing. Now, consider the case when the probability distribution of contending nodes differs from $p_{n_c,n}$. The probability of success in this case is smaller from the one calculated with the true probability distribution of contending nodes. Hence, it is interesting to measure the sensitivity of probability of success with γ. We also assume the number of nodes connected to bus, n_c, is a constant and can not be changed. Fig. 4.2 shows the probability of success as a function of γ, when optimum probabilities are calculated for $\gamma = 0.6$. It can be seen that the shape of the curve is similar to a logistic function and $\gamma = 0.6$ is in the

Algorithm 1 : Algorithm to minimize p_c with perfect sensing.

Set $\hat{U}(z) := \sqrt{G''(z)}$ /* $G''(z)$ is the second derivative of $G(z)$ with respect to z */
Initialization: Set $n := 2^{n_s}$, $N := 10\,n$, and $U_0 := 0$
for $i = 1$ to N **do**
    $U_i := U_{i-1} + \hat{U}\left(\frac{i-\frac{1}{2}}{N}\right)$
end for
Set $x_0 := 0$, and $x_n := 1$
for $t = 1$ to $n-1$ **do**
    $x_t = \frac{1}{N}\ \min\left\{i : \frac{U_i}{U_{N-1}} \geq \frac{t}{n}\right\}$
end for
Set $q := 1 - \frac{x\left(\frac{n}{2}\right)}{x(n)}$
for $l = 1$ to $n_s - 1$ **do**
    Set $L := 2^{n_s-l-1}$
    for $j = 0$ to 2^{l-1} **do**
        Convert j into l bits binary number c
        $q_c := \frac{x(2L(j+1))-x(L(2j+1))}{x(2L(j+1))-x(2Lj)}$
    end for
end for

middle part of the curve. We can also observe that the range of the changes in p_s is small, and therefore we can conclude that the performance of the protocol is almost independent of γ, when the optimum probabilities are calculated for $\gamma = 0.6$.

We now compare the performance of the selective tournaments scheme with CDR under perfect carrier sensing. To make a fair comparison, we note that, with the same number of slots, both schemes increase the packet overhead by the same length. We plotted the probability of success as a function of n_c, number of nodes connected to the bus, for different number of slots in Fig. 4.3. We have also assumed the number of contending nodes, for both schemes, follows the probability distribution given in (5.1) for γ= 0.6. It can be observed that the selective tournaments with six slots has a much better performance than CDR scheme with five, seven, and nine slots, and still a higher probability of success than CDR with eleven slots.

Table 4.1: Optimal parameters for (n_c=16, n_s=6, γ=0.6)

$q = 0.189$	$q_{0110} = 0.483$	$q_{01011} = 0.5$
$q_0 = 0.279$	$q_{0111} = 0.481$	$q_{01100} = 0.5$
$q_1 = 0.396$	$q_{1000} = 0.5$	$q_{01101} = 0.466$
$q_{00} = 0.371$	$q_{1001} = 0.473$	$q_{01110} = 0.5$
$q_{01} = 0.4$	$q_{1010} = 0.47$	$q_{01111} = 0.461$
$q_{10} = 0.438$	$q_{1011} = 0.466$	$q_{10000} = 0.454$
$q_{11} = 0.458$	$q_{1100} = 0.5$	$q_{10001} = 0.454$
$q_{000} = 0.434$	$q_{1101} = 0.5$	$q_{10010} = 0.5$
$q_{001} = 0.438$	$q_{1110} = 0.454$	$q_{10011} = 0.444$
$q_{010} = 0.448$	$q_{1111} = 0.545$	$q_{10100} = 0.444$
$q_{011} = 0.465$	$q_{00000} = 0.486$	$q_{10101} = 0.5$
$q_{100} = 0.463$	$q_{00001} = 0.475$	$q_{10110} = 0.5$
$q_{101} = 0.468$	$q_{00010} = 0.49$	$q_{10111} = 0.428$
$q_{110} = 0.461$	$q_{00011} = 0.489$	$q_{11000} = 0.428$
$q_{111} = 0.5$	$q_{00100} = 0.5$	$q_{11001} = 0.571$
$q_{0000} = 0.458$	$q_{00101} = 0.472$	$q_{11010} = 0.5$
$q_{0001} = 0.46$	$q_{00110} = 0.484$	$q_{11011} = 0.5$
$q_{0010} = 0.461$	$q_{00111} = 0.5$	$q_{11100} = 0.5$
$q_{0011} = 0.459$	$q_{01000} = 0.5$	$q_{11101} = 0.6$
$q_{0100} = 0.458$	$q_{01001} = 0.5$	$q_{11110} = 0.4$
$q_{0101} = 0.461$	$q_{01010} = 0.476$	$q_{11111} = 0.5$

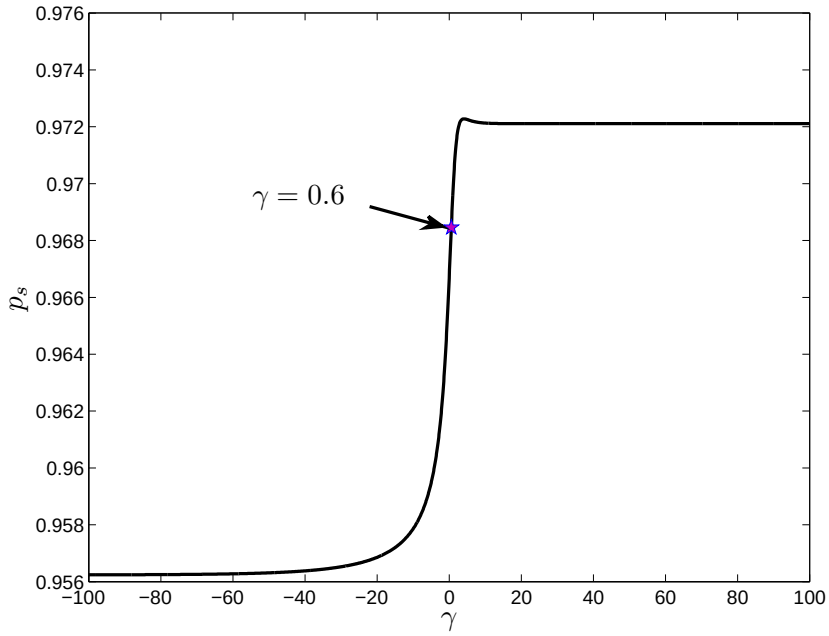

Figure 4.2: p_s as a function of γ, when the optimal probabilities are obtained for γ=0.6 (perfect sensing).

4.3.2 Throughput and Delay Analysis

We define the network throughput ρ as a ratio of time occupied by the transmitted packet to the total medium access time for successfully transmitting a packet as

$$\rho = \frac{p_s T_{pkt}}{p_s T_s + p_c T_c + p_i T_i} \tag{4.10}$$

where T_{pkt} is the time to transmit a packet. T_s and T_c denote the time taken by a successfully and a collided transmission, respectively, and T_i is the time consumed by an idle cycle.

We can also derive the average delay for a successful transmitted packet, which is defined as a time spent from the moment that the packet reaches the head-of-line of the queue to the time that it is transmitted successfully. Assume a given node has a

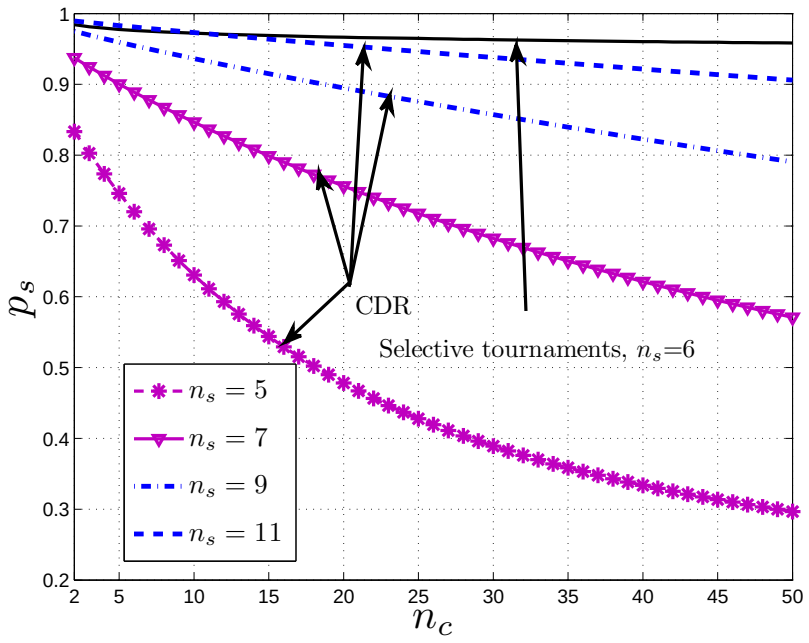

Figure 4.3: Probability of success for selective tournaments and CDR versus n_c for different number of slots (perfect sensing).

packet to send, the probability that it wins the contention is given by

$$p_s^\star = \sum_{k=2}^{n_c} \frac{p_s^\delta(k)}{k}\, p_{n_c,k} \tag{4.11}$$

where $p_s^\delta(k)$ is the probability of successful data transmission calculated in (5.18) for $p_{n_c,n} = \delta(n-k)$, and $\delta(.)$ denotes the dirac delta function. Note that the optimal probabilities are still calculated using Algorithm 1 with $p_{n_c,n}$ given in (5.1). However, we are evaluating the success probability with $\delta(n-k)$ since we are interested in the case when exactly k nodes are contending for the medium. For a given node, the probability that a successful transmission is followed by j fails is $p_s^\star(1-p_s^\star)^j$, and

thus the average delay is expressed by

$$D = \sum_{j=0}^{\infty} p_s^\star (1 - p_s^\star)^j (T_s + jT_{avg}) = T_s + \frac{T_{avg}}{p_s^*} \tag{4.12}$$

where T_{avg} is the average transmission time, and is given by

$$T_{avg} = p_s T_s + p_c T_c + p_i T_i \tag{4.13}$$

4.4 Numerical Results

In this section, we evaluate the MAC layer throughput and delay as a function of physical layer sensing errors. We assume the following parameters for our evaluations. Physical layer bit rate is set to 1Mbps, and the sampling rate of the ADC is 500kHz. The packet has a payload size of 14 bytes [14]. We also assume the preprocessor introduced in Chapter 2 can completely remove the impulses from received signal, and therefore we obtain the results under Gaussian noise assumption. Throughout this section, the number of slots is fixed to 6, and n_c and γ in (5.1) are set to 16 and 0.6, respectively, unless specified otherwise.

The effect of false alarm error on the network throughput is illustrated in Fig. 4.4. The number of samples taken from the signal is set to 10, which is twice the time-bandwidth product. The SNR varies from -5dB to 5dB. As can be seen, for a fixed SNR, there is an optimum false alarm error that maximizes the throughput. It can also be observed that as SNR increases, the optimum point moves to the left, and therefore maximum throughput is achieved with smaller values of false alarm errors. When we increase the false alarm error from its optimum value, the throughput degrades at a much higher rate for higher SNR values. Hence, it is crucial to find the

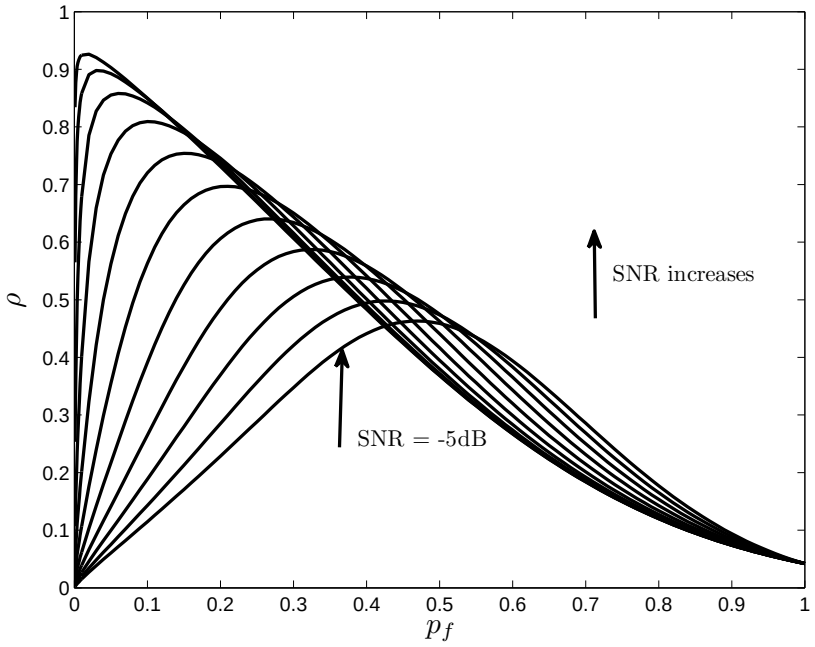

Figure 4.4: ρ versus p_f for different SNR values, $u = 5$.

optimum value for false alarm error which maximizes the network throughput.

Figs. 4.5-4.7 show the behavior of network throughput, delay, and false alarm error as a function of SNR for different number of samples. Fig. 4.5 shows the false alarm errors that maximize the network throughput. We obtained these values by numerically evaluating (2.6), (2.7), and (4.10). It can be observed that for a fixed number of samples, the optimum p_f decreases as SNR increases, and for a fixed SNR, as number of samples increases, the optimal p_f decreases. Fig. 4.6 plots the maximum throughput achieved by using the optimal values of p_f obtained from Fig. 4.5. The interesting observation is that the network throughput decreases as number of samples increases in low SNR regions. The reason is as follows. As we increment u, false alarm error decreases, while miss detection error decreases slightly and remains high, and results in an increase in the value of collision probability. Moreover, the network throughput decreases as the slot time increases, and thus reduces the value

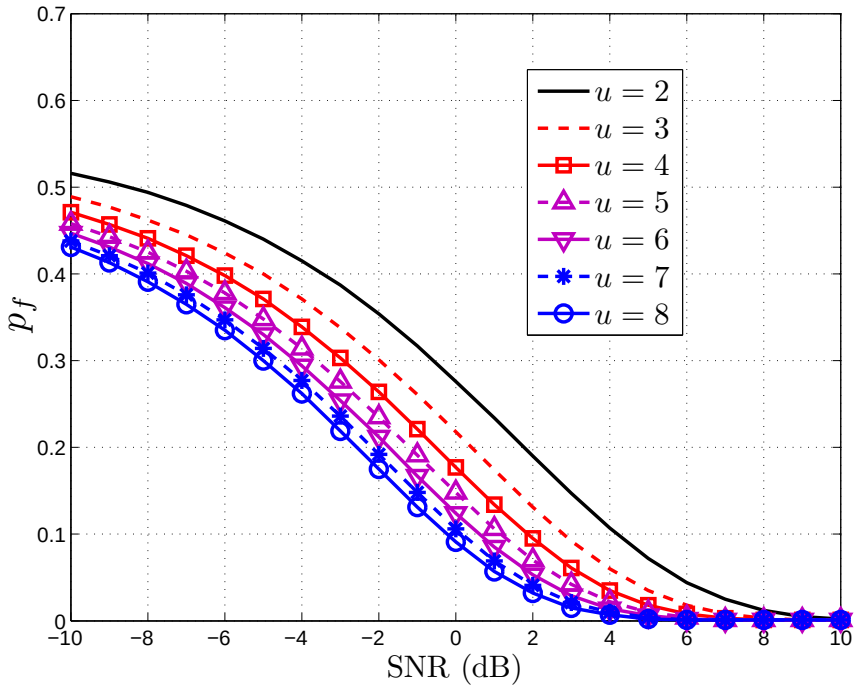

Figure 4.5: Optimum false alarm error versus SNR for different values of u.

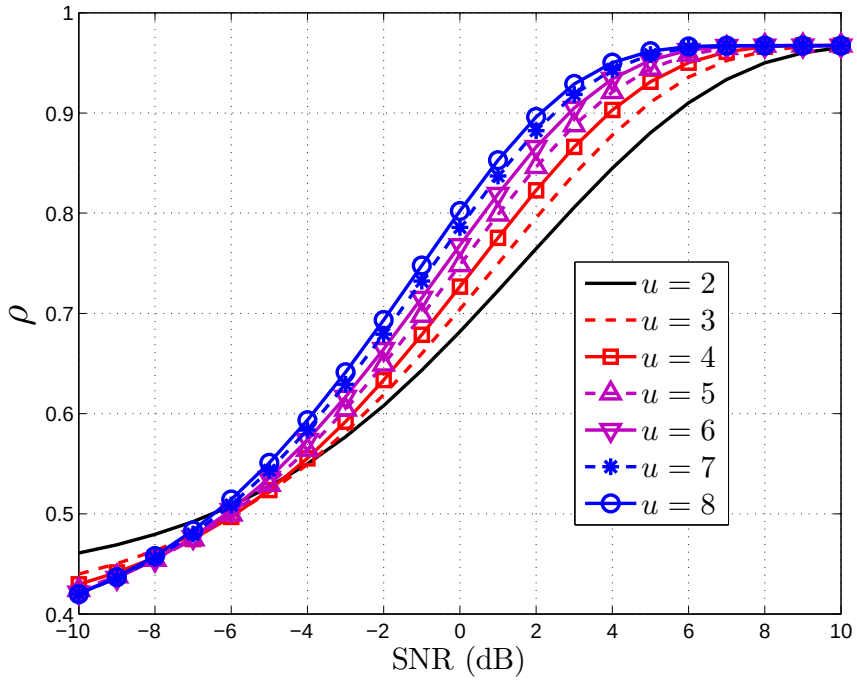

Figure 4.6: Maximum throughput as a function of SNR for different values of u.

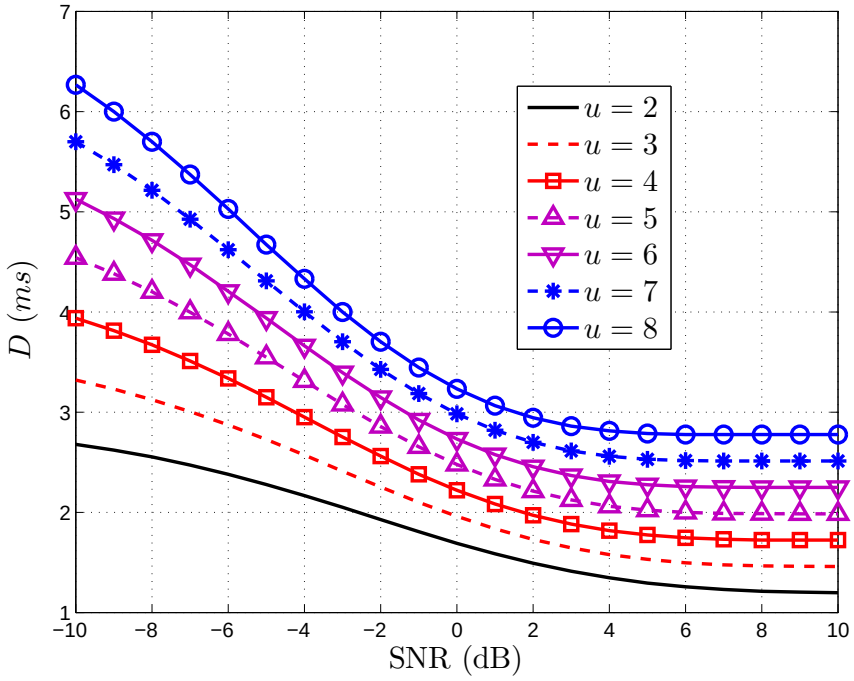

Figure 4.7: Network delay versus SNR for different values of u.

of throughput. Finally, Fig. 4.7 illustrates the effect of the throughput maximization on the average packet delay. One can observe that for a fixed number of samples, as the optimum value of p_f decreases, the average delay increases.

4.5 Summary

In this chapter, we have extended the analysis of a contention-based MAC protocol, called selective tournaments, suitable for in-vehicle PLC, under carrier sensing errors. We have shown that the selective tournaments significantly outperforms CDR, the contention-based MAC protocol proposed for in-vehicle PLC. We have obtained the network throughput and delay as a function of physical layer sensing errors: false alarm and miss detection. We have shown that the behavior of throughput depends on the false alarm and miss detection errors. We have also obtained the false alarm

errors that maximize the throughput using numerical methods in different scenarios, and showed the effect of those variables on the network delay.

Chapter 5

Multi-channel Contention Resolution Algorithm with Imperfect Carrier Sensing

In the previous two chapters, we have introduced two random access protocols for V-PLC systems. The first protocol resolved the contention in the frequency-domain, and the second protocol resolved the contention using a robust CSMA-like approach. In this chapter, we introduce a new MAC protocol that uses a combination of the techniques used in the previous two protocols to resolve the contention. We first present our system model and give a brief description of the MAC protocol operation in Section 5.1. Section 5.2 provides mathematical analysis of the proposed MAC protocol, under the assumption of perfect sensing, whereas in Chapter 5.3, we present the mathematical analysis of the protocol with the presence of sensing errors. We present numerical results in Section 5.4, and summarize in Section 5.5.

5.1 System Model

We consider a V-PLC network in which N nodes are connected to the harness. Time is divided into a fixed-size transmission cycles, where multiple frequency channels can be used by the senders or receivers. Despite the using of multiple channels, we assume

that each node including the receiver, has only one antenna. We further assume all nodes in the V-PLC network are time synchronized. Fig. 5.1 depicts the structure of a single transmission cycle. First, the contention between senders is resolved on the frequency domain where each sender, at the beginning of the transmission cycle, picks up a channel randomly. Then, if more than one sender select the same channel, the contention is resolved over number of slots by randomly perform one of the two following actions in each slot: a carrier sense (cs) operation or a carrier transmission (ct) operation. At each time slot, the sender defers its transmission to the next transmission cycle if it senses the channel busy. But if the sender does not hear the carrier, it stays on the contention. At the end of the last slot, the remaining senders transmit a long preamble on their selected channel. After that the receiver starts sampling the signal level on each channel starting with the channel 1, and if detects any valid carriers, it locks on the channel and waits to receive the packet. Note that the procedure performed on each channel is the contention resolution algorithm proposed in Chapter 4, and the channel selection algorithm is the same scheme as the one introduced in Chapter 3.

5.2 Performance Analysis under Perfect Sensing

Consider a system scenario, where at a given time, n nodes try to transmit packets over the dc power line. We assume the value of n is not known to the nodes, but its

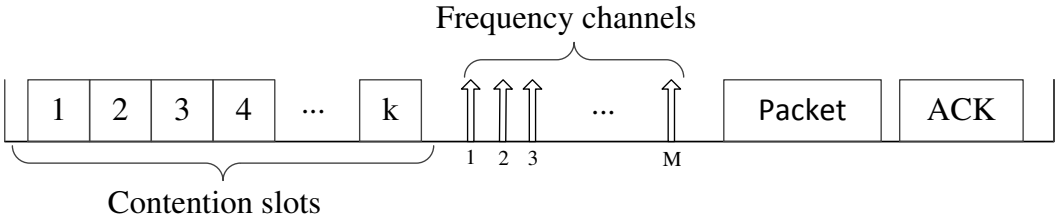

Figure 5.1: A view of a single transmission cycle.

probability mass function is known to all nodes in the network, and can be expressed as

$$p_N(n) = \frac{1}{\zeta(\gamma) n^{\gamma}} \tag{5.1}$$

where $n \in \{2, \ldots, N\}$, N is the number of nodes connected to the dc-bus, and $\zeta(\gamma) = \sum_{z=2}^{N} \frac{1}{z^{\gamma}}$, where γ is the shape parameter of the distribution.

We are now ready to formulate the problem. Let $\mathbf{p} = (p_1, p_2, \ldots, p_M)$ be the channel selection distribution, where p_m is the probability that the m-th channel is selected by a sender. Assume the collision resolution algorithm uses k slots, and let $q^{(m)}$ be the probability vector of size $\sum_{i=0}^{k-1} 2^i = 2^{k-1}$, used to resolve the contention on the m-th channel. Therefore, the probability vectors on all M channels can be expressed with a matrix $\mathbf{q} = [q^{(1)}, q^{(2)}, \ldots, q^{(M)}]^T$. Suppose the number of senders in the contention is n. A transmission cycle is successful if the contention is successfully resolved in the first non-idle frequency channel, thus, the success probability is given by

$$\pi_p(n) = \sum_{m=1}^{M} \prod_{t=0}^{m-1} (1 - p_t)^n \sum_{i=1}^{n} \binom{n}{i} (p_m)^i (1 - p_m)^{n-i} \tau_{q^{(m)}}(i) \tag{5.2}$$

where $p_0 := 0$, and $\tau_{q^{(m)}}(i)$ is the probability that the contention is successfully resolved on the m-th channel when i nodes selected that channel. Averaging $\pi_p(n)$ over the distribution described in (5.1), the average success probability can be written as

$$\pi_p = \mathbb{E}[\pi_p(n)] = \sum_{n=2}^{N} p_N(n) \pi_p(n) \tag{5.3}$$

Furthermore, in order to calculate $\tau_{q^{(m)}}$, we need to find the probability mass function of the number of contending nodes on the m-th channel. For a given vector

p, this distribution can be expressed as

$$p_N^{(m)}(l) = \sum_{n=l}^{N} \binom{n}{l} (p_m)^l (1-p_m)^{n-l} p_N(n) \tag{5.4}$$

where $m \in \{1, \ldots, M\}$ and $l \in \{0, \ldots, N\}$. We need to find the values in the vector **p** that provide fast collision resolution. For this purpose, we have chosen the truncated geometric distribution used in the design of Sift protocol [16]. Sift is a randomized carrier sense multiple access- (CSMA-) based protocol for wireless sensor networks, where nodes use a truncated geometric distribution for selecting their contention slots. Similarly, in our protocol, senders use this geometrically-increasing probability distribution for picking their channels in the transmission cycle. Its expression for $m = 1, \ldots, M$ is given by

$$p_m = \frac{\beta^{\frac{m}{M}} - \beta^{\frac{m-1}{M}}}{\beta - 1} \tag{5.5}$$

where β is the parameter that needs to be carefully designed. Fig. 5.2 illustrates the impact various values of β have on the channel probabilities when $M = 10$ channels are used. We have obtained these probabilities for three values of β; $\beta = 10$, $\beta = 100$, and $\beta = 1000$. It can be observed that the channel probabilities increase much faster as β increases.

Now, we try to find the probability distribution **p** and matrix **q** that maximize the success probability described in (5.3), i.e.,

$$\arg\max_{\mathbf{p},\mathbf{q}} \pi_p \tag{5.6}$$

Algorithm 2 describes how we can calculate the optimal vector $q^{(m)}$ for the m-th channel, given the distribution of contenders on the m-th channel, i.e., the value of p_m is assumed to be known. We have used the method proposed in [13] to minimize

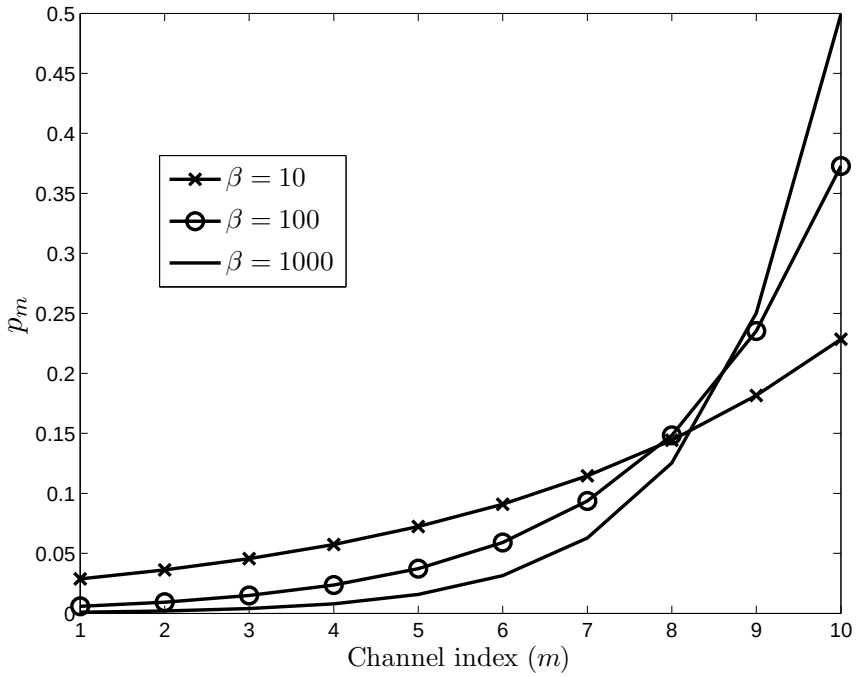

Figure 5.2: Channel selection probabilities when $M = 10$ channels are available for multiple choices of β.

the collision probability on the m-th channel, which finds the optimum solution by approximating the collision probability with a Riemann integral. Using Algorithm 2 and (5.5), the optimization problem in (5.6) can be solved by numerical methods [17].

Suppose that the random variable T_1 denotes the number of transmission cycles required to successfully transmit the first packet. If there are n contenders, then

$$\mathbb{P}(T_1 = r) = \pi_p(n)(1 - \pi_p(n))^{r-1} \tag{5.7}$$

where $r \in \{1, 2, \dots\}$, and $\pi_p(n)$ is the probability of success described in (5.2) when there are n contenders. Note that T_1 describes the delay correspond to the first packet successfully transmitted to the receiver. By a similar argument, we find the distribution of T_w, the number of transmission cycles needed to transmit w packets

Algorithm 2 : Algorithm to maximize success probability on the m-th frequency channel.

Set $\hat{u}(z) := \sqrt{g''(z)}$ /* $g''(z)$ is the second derivative of $g(z) = \sum_{n=2}^{N} p_N^{(m)}(n) z^n$ with respect to z */
Initialization: Set $b := 2^k$, $B := 10\,b$, and $u_0 := 0$
for $i = 1$ to B **do**
    $u_i := u_{i-1} + \hat{u}\left(\frac{i-\frac{1}{2}}{B}\right)$
end for
Set $x_0 := 0$, and $x_b := 1$
for $t = 1$ to $b-1$ **do**
    $x_t = \frac{1}{B}\ \min\left\{i : \frac{u_i}{u_{B-1}} \geq \frac{t}{b}\right\}$
end for
Set $q^{(m)} := 1 - \frac{x\left(\frac{b}{2}\right)}{x(b)}$
for $L = 1$ to $k-1$ **do**
    Set $L := 2^{k-l-1}$
    for $j = 0$ to 2^{l-1} **do**
        Convert j into l bits binary number c
        $q_c^{(m)} := \frac{x(2L(j+1)) - x(L(2j+1))}{x(2L(j+1)) - x(2Lj)}$
    end for
end for

to the destination. Let X_i denote the number of transmission cycles required to transmit the i-th packet, conditioned that the previous packets have been transmitted successfully. Form (5.7), it is obvious that X_i has a geometric distribution with average $\frac{1}{\pi_p(n-i+1)}$. We can express the random variable T_w as

$$T_w = \sum_{i=1}^{w} X_i \tag{5.8}$$

Thus, the expected value of T_w is

$$\mathbb{E}[T_w] = \sum_{i=n-w+1}^{n} \frac{1}{\pi_p(i)} \tag{5.9}$$

with $w \in \{1, 2, \ldots, n\}$. The normalized throughput under consideration in this paper is defined as a fraction of time the network is used to successfully transmit packets.

We define the throughput correspond to the w-th received packet as the ratio

$$\rho_w(n) = \frac{w\sigma_d}{\mathbb{E}[T_w]\sigma_{cycle}} \tag{5.10}$$

with the transmission cycle duration is defined as $\sigma_{cycle} = k\sigma_s + M\sigma_c + \sigma_d$, where σ_s represents the amount of time required by a node to determine the presence of the carrier on a frequency channel, σ_c is the time duration needed by the receiver to sample a frequency channel and switch to the next channel, and σ_d specifies the amount of time needed for transmitting a packet and receiving an ACK.

5.3 Performance Analysis under the Presence of Sensing Errors

Suppose there are N nodes connected to the dc power line network and the number of nodes with packets follows the distribution described in (5.1). Furthermore, assume that sensing is not perfect, and there are sensing errors due to the channel impairments. Let $p_{fa}^{(m)}$ and $p_{md}^{(m)}$ denote the false alarm and miss-detection probabilities for senders on the m-th channel, respectively. Similarly, we define $q_{fa}^{(m)}$ and $q_{md}^{(m)}$ as the probabilities of false alarm and miss-detection related to the receiver on the m-th channel, respectively. We also use the signal detector introduced in Chapter 2 for signal detection. Next, we calculate the success probability when there are n contenders. Assume m is the channel selected by at least one node. We say that the contention is successfully resolved on the m-th channel if and only if: (i) only one node remains on the m-th channel after the completion of the collision resolution protocol. (ii) the receiver is able to correctly determine the states of the first m

channels. Hence, the success probability can be expressed as

$$\pi_p(n) = \sum_{m=1}^{M} (1 - q_{md}^{(m)}) \prod_{t=0}^{m-1} (1 - p_t)^n (1 - q_{fa}^{(t)}) \sum_{i=1}^{n} \binom{n}{i} (p_m)^i (1 - p_m)^{n-i} \tau_{q^{(m)}}(i, p_{fa}^{(m)}, p_{md}^{(m)}) \tag{5.11}$$

where $p_0 := 0$, $p_{fa}^{(0)} := 0$, and the expected value of success probability is expressed by (5.3).

Next, we derive the success probability, $\tau_{q^{(m)}}$, on the m-th channel when sensing is not perfect. We define the probability generating function (PGF) of the number of contending nodes on the m-th channel as

$$g^{(m)}(z) := \mathbb{E}(z^n) = \sum_{n=0}^{N} p_N^{(m)}(n)\ z^n \tag{5.12}$$

We are now able to find the PGF of the number of contenders still in the competition after the elapse of one time slot. For simplicity of computation, we assume that, by using the preprocessor suggested in Chapter 2, all nodes in the competition experience the same average SNR and therefore, we can use binomial distribution to denote the probability that i out of n nodes estimated the channel state correctly. Because this PGF depends on the number of nodes who selected ct operation in the previous slot, we derive its expression for the following cases:

- Case 1: If no carrier has been emitted in the first slot, then a node moves to the second slot if it senses the channel idle, which happens with probability $1 - p_{fa}$.

The PGF denoted as $g_0^{(m)}$, is given as

$$\begin{aligned} g_0^{(m)}(z) &= \sum_{n=0}^{N} p_N^{(m)}(n) \left(1-q^{(m)}\right)^n \sum_{i=0}^{n} \binom{n}{i} \left(1-p_{fa}^{(m)}\right)^i \left(p_{fa}^{(m)}\right)^{n-i} z^i \\ &= \sum_{n=0}^{N} p_N^{(m)}(n) \left(1-q^{(m)}\right)^n \left(\left(1-p_{fa}^{(m)}\right) z + p_{fa}^{(m)}\right)^n \\ &= g^{(m)}\left((1-q^{(m)}) z_{fa}^{(m)}\right) \end{aligned} \tag{5.13}$$

where $z_{fa}^{(m)} := \left(1-p_{fa}^{(m)}\right) z + p_{fa}^{(m)}$, $q^{(m)}$ is the probability of transmitting a carrier in the first time slot, and $p_{fa}^{(m)}$ is the false alarm probability on the m-th channel given in (2.7).

- Case 2: In this case, we consider scenarios where at least one node has emitted a carrier in the previous slot. All nodes in the contention that have emitted a carrier in the first slot survive and move to the second time slot. However, nodes that have sensed the channel busy, which happens with probability $1-p_{md}$ will retire from contention. Others that have miss-detected the carrier on the channel, will continue the contention. Therefore, the expression for its PGF, $g_1^{(m)}$, is expressed by

$$\begin{aligned} g_1^{(m)}(z) =& \sum_{n=1}^{N} p_N^{(m)}(n) \sum_{i=1}^{n} \binom{n}{i} \left(q^{(m)}\right)^i \left(1-q^{(m)}\right)^{n-i} z^i \\ & \sum_{j=0}^{n-i} \binom{n-i}{j} \left(p_{md}^{(m)}\right)^j \left(1-p_{md}^{(m)}\right)^{n-i-j} z^j \\ &= g^{(m)}\left(q^{(m)} z + (1-q^{(m)}) z_{md}^{(m)}\right) - g^{(m)}\left((1-q^{(m)}) z_{md}^{(m)}\right) \end{aligned} \tag{5.14}$$

where $z_{md}^{(m)} := p_{md}^{(m)} z + 1 - p_{md}^{(m)}$, and $p_{md}^{(m)}$ is the miss detection probability on the m-th channel defined in (2.6).

Let $c = [c_1 \dots c_i \dots c_t]$ be an t-bit binary number that shows the operations performed by a sender in each slot, where $c_i = 0$ or 1 denotes the events of choosing cs and ct in the i-th slot, respectively. We are now able to find the PGF of the nodes in the contention after the elapse of $t+1$ slots. Following mathematical induction and using (5.13) and (5.14), we have

$$g_{c0}^{(m)}(z) = g_c^{(m)}\left((1-q_c^{(m)})z_{fa}^{(m)}\right) \tag{5.15}$$

and

$$g_{c1}^{(m)}(z) = g_c^{(m)}\left(q_c^{(m)}z + (1-q_c^{(m)})z_{md}^{(m)}\right) - g_c^{(m)}\left(\left(1-q_c^{(m)}\right)z_{md}^{(m)}\right) \tag{5.16}$$

where $q_c^{(m)}$ is the probability that, in slot $t+1$, nodes emit a carrier on the m-th channel, given the signaling pattern c in the first t slots, $g_c^{(m)}$ is the PGF of survivors, when the signaling pattern in the first t slots is c, and $g_{\varnothing}^{(m)} := g^{(m)}$. Hence, the PGF of the number of contenders on the m-th channel after k slots is $\sum_{c\in\mathcal{C}_k} g_c^{(m)}(z)$, where $\mathcal{C}_k$ denotes the set of all binary numbers of length k from the alphabet $\{0,1\}$. So the distribution of survivors is given by

$$\Pr\{\text{n nodes remain on the m-th channel}\} = \frac{1}{n!}\frac{d^n}{dz^n}\sum_{c\in\mathcal{C}_k} g_c^{(m)}(z)|_{z=0} \tag{5.17}$$

where n denotes the number of survivors at the end of the contention. The success probability, which is defined as the probability that at the end of the contention only one survivor remains, is given as

$$\tau_{q^{(m)}} = \frac{d}{dz}\sum_{c\in\mathcal{C}_k} g_c^{(m)}(z)|_{z=0} \tag{5.18}$$

5.4 Numerical Results

In this section, we present numerical results obtained by evaluating the expressions derived in Sections 5.2 and 5.3 to illustrate the performance of the proposed protocol. Throughout this section we assume the number of nodes connected to the dc power line, N, is 50, and the shape parameter of the distribution in (5.1) is set to 0.6, unless specified otherwise. The reason behind choosing $\gamma = 0.6$ is that the system will perform well in both high and low traffic loads as shown in Fig. 5.3. Here, there are $N = 50$ nodes connected to the harness, and the system uses $M = 2$ channels and $k = 6$ slots to resolve the contention between nodes. It can be noted that the system with $\gamma = 0$ (uniform distribution) performs well when the number of contenders is large, whereas the system with $\gamma = 1$ gives a better performance when the number of contending nodes is small, and the system with $\gamma = 0.6$ provides a good performance in both cases. Our experiments confirm that $\gamma = 0.6$ provides a balanced performance for other configurations as well, i.e., different values of M and k.

Figs. 5.4 and 5.5 show the success probability and the system throughput as the number of channels varies between 2 and 8 for different number of contention slots, respectively. To evaluate the effects of the number of frequency channels and contention slots on the system throughput, we define a ratio between time constants in each transmission cycle as $r := \frac{\sigma_s}{\sigma_d} = \frac{\sigma_c}{\sigma_d}$. Here, we considered that $\sigma_s = \sigma_c$, however, the case of $\sigma_s \neq \sigma_c$ can be easily included in the numerical evaluations as well. Expectedly, as can be observed in Fig. 5.4, with an increase in the number of contention slots or frequency channels, the success probability of the protocol increases. However, as the number of contention slots increases, the gain of using multiple frequency channels decreases since the protocol is capable of resolving the contention on each channel with a high probability. In Fig. 5.5, we assume that the

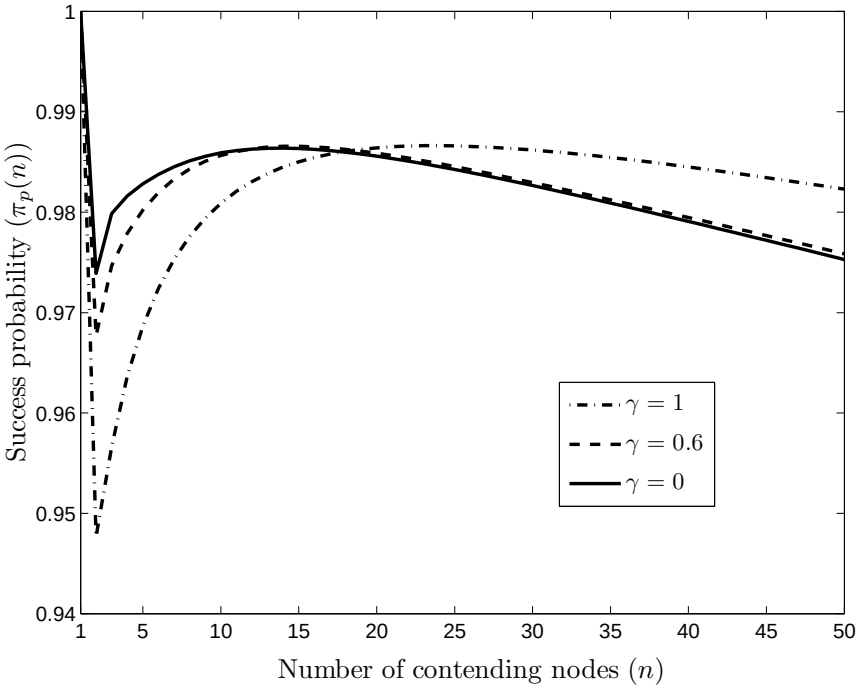

Figure 5.3: Success probability versus number of contending nodes for different values of γ, $N = 50$, $k = 6$, $M = 2$.

packet size is relatively large, and therefore $r = \frac{1}{60}$. Each point describes the expected throughput computed as $\sum_{n=2}^{N} p_N(n)\rho_1(n)$, and the maximum point along each curve is specified with a marker. We can observe that, as the number of contention slots increases, the maximum point along each curve moves to the left and thus, occurs at a smaller number of channels. It can also be seen that adding a channel to the system does not improve the system performance when number of contention slots used in the system is high. The reason behind this behavior is that the system with large k can handle a wide range of traffic loads, and therefore the success probability will not improve much by separating contenders across more channels. On the other hand, adding one channel will increase the packet overhead and thus, could potentially degrade the system performance.

Fig. 5.6 shows the average success probability of the system as a function of the network size. The protocol operational parameters (k, M) are set to the values give

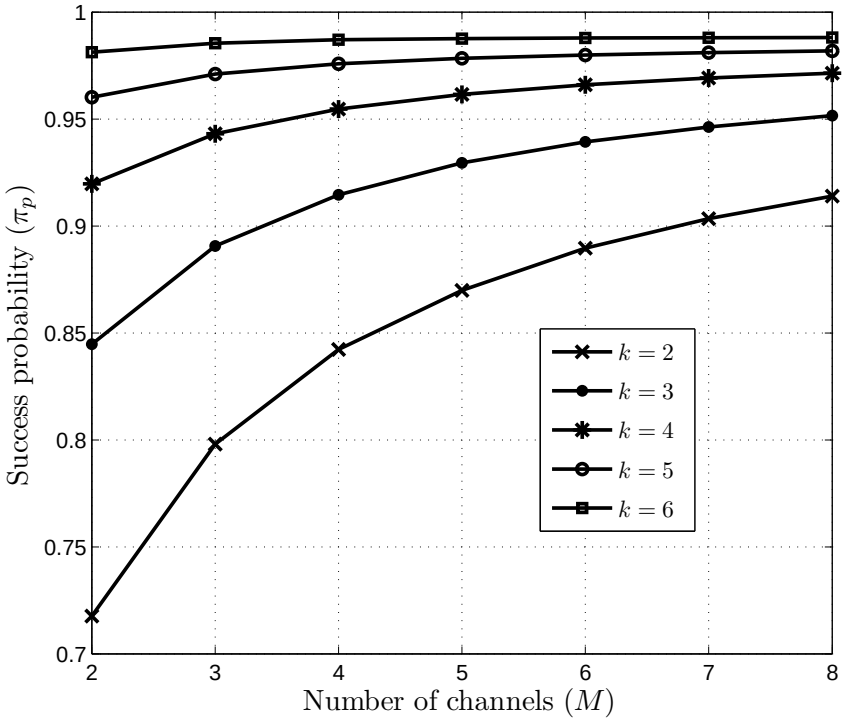

Figure 5.4: Average success probability versus number of channels for different number of time slots (k), $N = 50$, $\gamma = 0.6$.

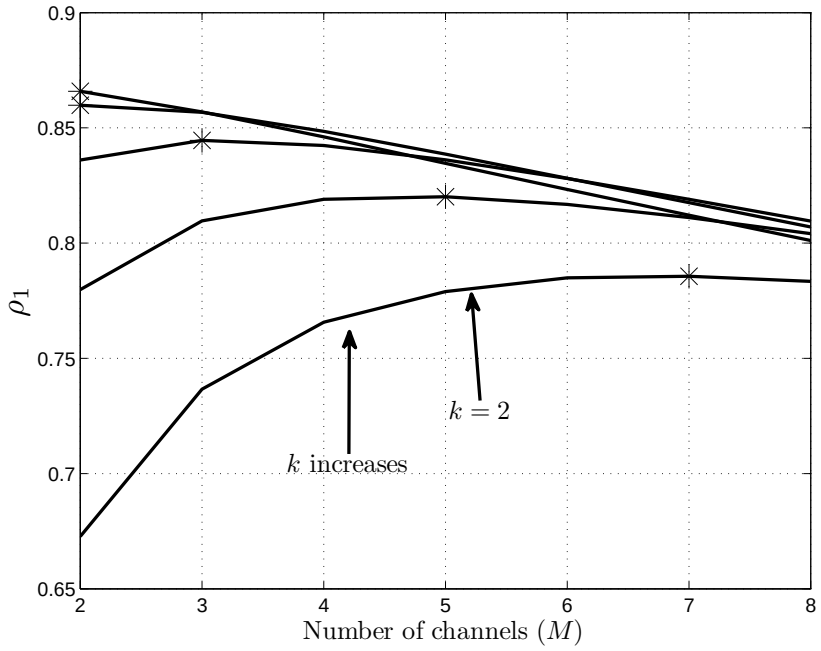

Figure 5.5: ρ_1 versus number of channels for different number of time slots (k), $N = 50$, $\gamma = 0.6$.

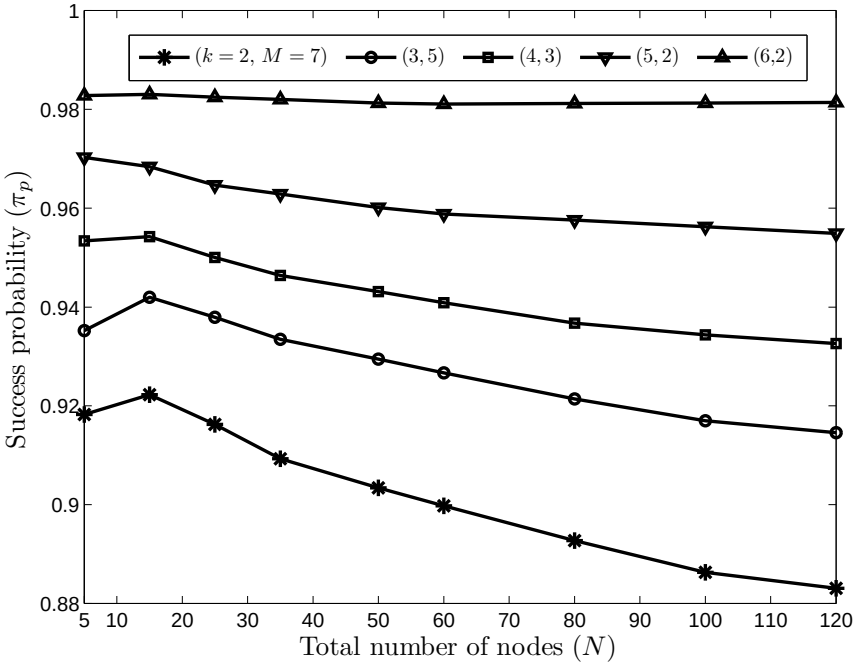

Figure 5.6: The average success probability versus total number of nodes connected to the harness (N), $\gamma = 0.6$.

the maximum throughput as shown in Fig. 5.5. It could be noticed that the system shows the least performance degradation when $k = 6$ and $M = 2$. The reason is that as we increase the number of contention slots in each channel, the collision resolution algorithm performed on each channel is more capable of resolving the contention in a wide range of traffic loads, and also less sensitive to the number of contenders compared to the channel selection algorithm.

In Figs. 5.7-5.10, we report the probability mass functions of the number of transmission cycles required to transmit the first and all packets, when there are 25 and 5 contenders. We assume there are $k = 4$ slots available on each channel to resolve the contention, and the system uses $M = 3$ channels as according to Fig. 5.5, this configuration provides the highest throughput when $k = 4$. We have plotted theses distributions by using (5.8), and the results obtained by solving the optimization problem given in (5.6). The figures show that the protocol delivers the packets with

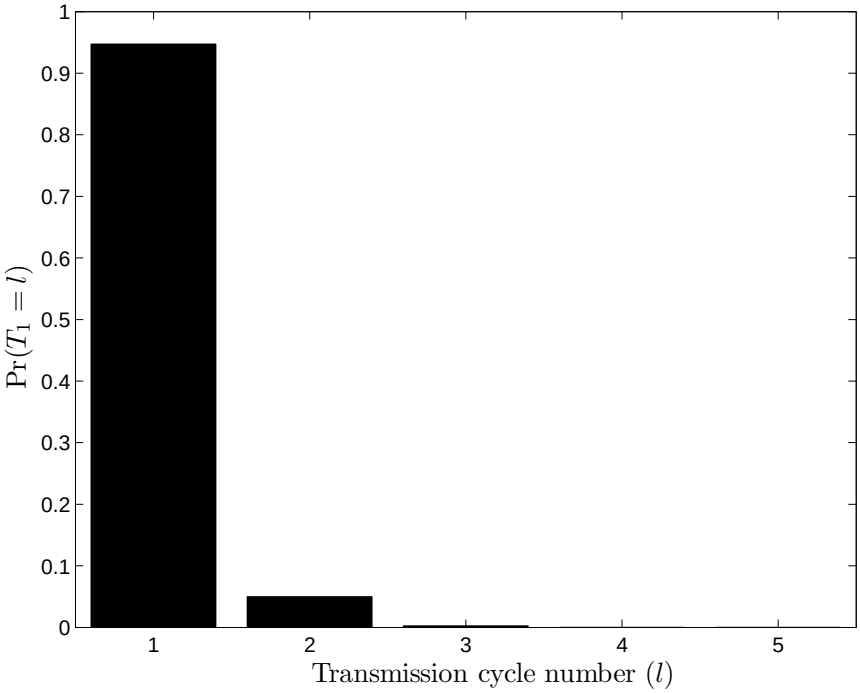

Figure 5.7: Probability mass function of the number of transmission cycles required to transmit the first packet when there are 25 contenders, $N = 50$, $\gamma = 0.6$, $k = 4$, $M = 3$.

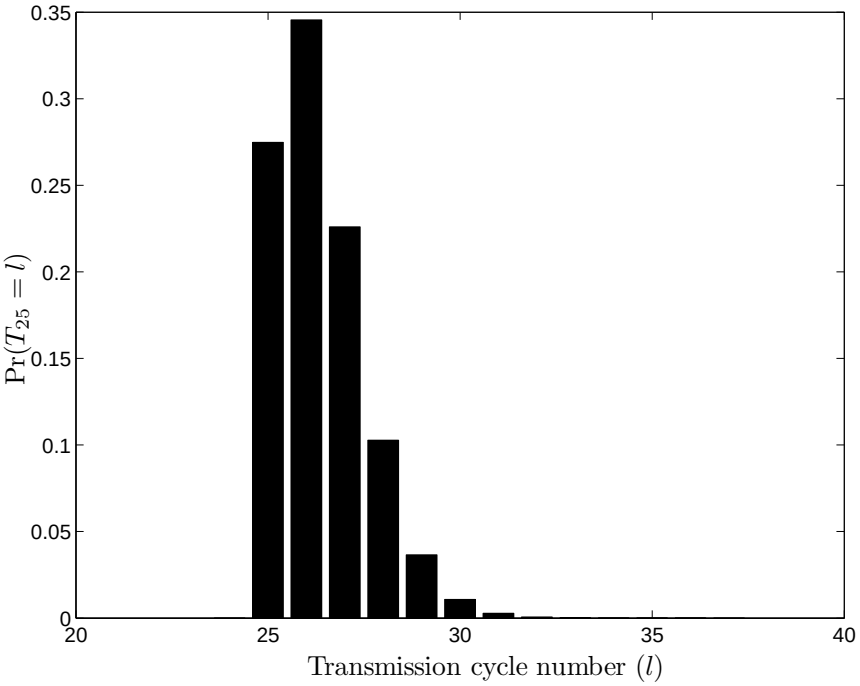

Figure 5.8: Probability mass function of the number of transmission cycles required to transmit all packets when there are 25 contenders, $N = 50$, $\gamma = 0.6$, $k = 4$, $M = 3$.

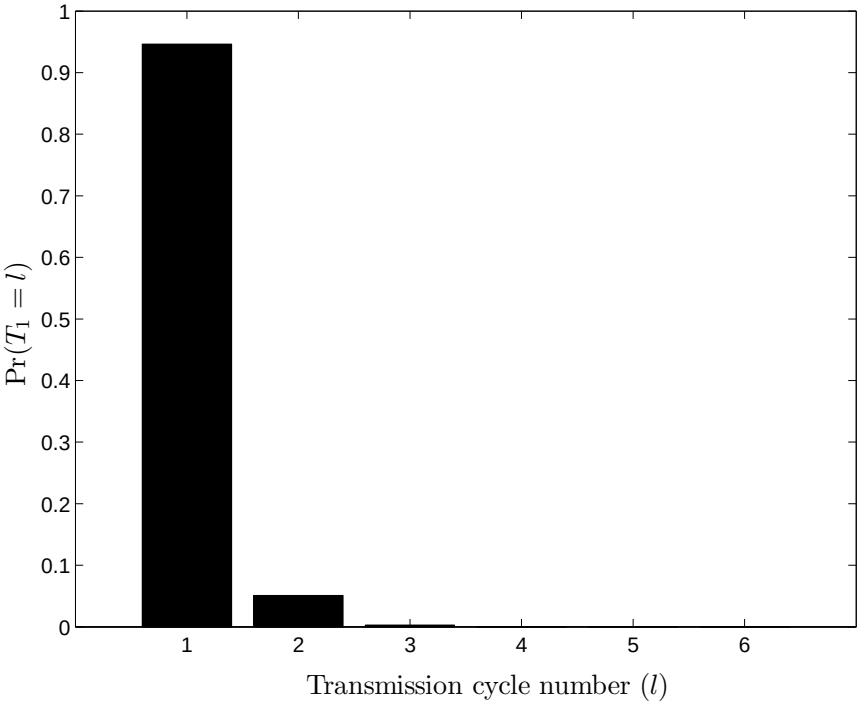

Figure 5.9: Probability mass function of the number of transmission cycles required to transmit the first packet when there are 5 contenders, $N = 50$, $\gamma = 0.6$, $k = 4$, $M = 3$.

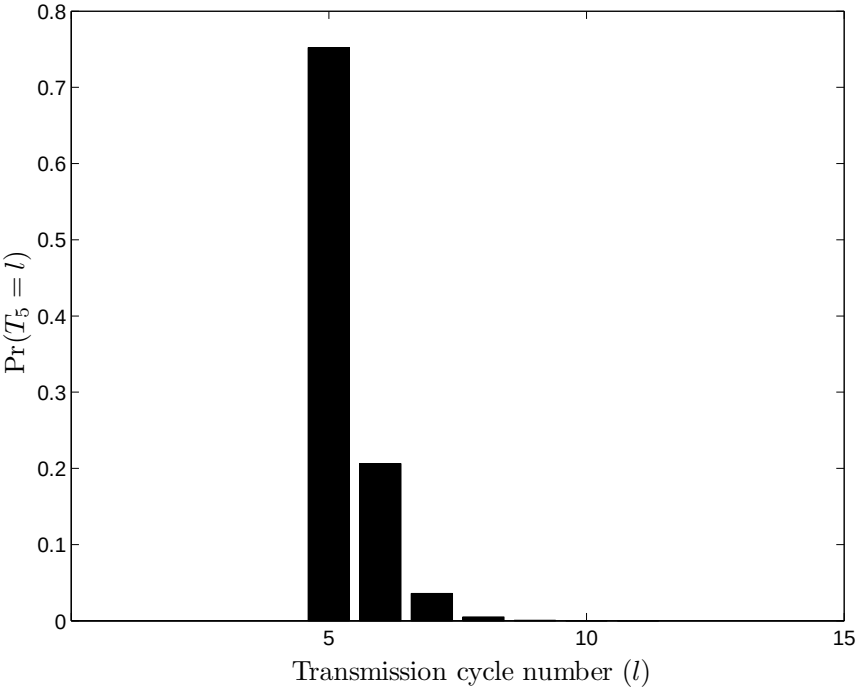

Figure 5.10: Probability mass function of the number of transmission cycles required to transmit all packets when there are 5 contenders, $N = 50$, $\gamma = 0.6$, $k = 4$, $M = 3$.

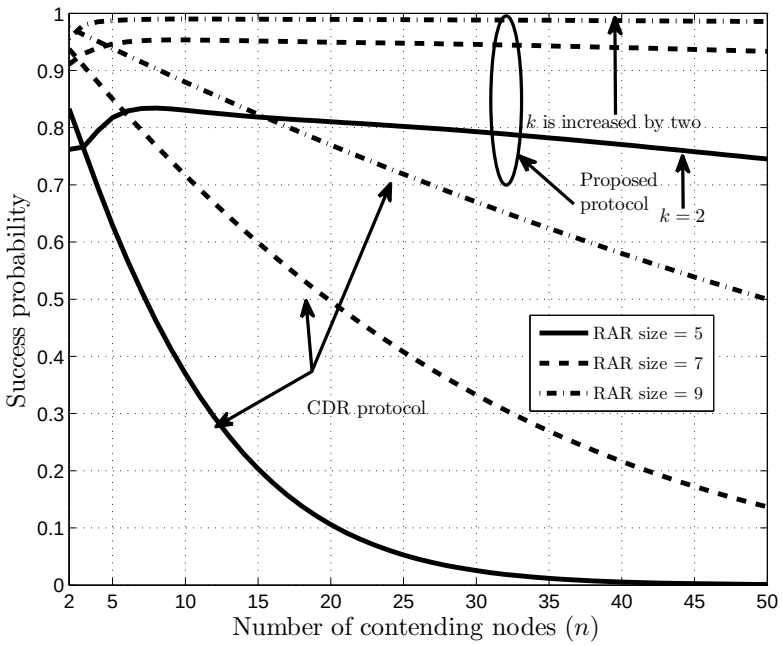

Figure 5.11: Success probability of the proposed protocol and CDR versus number of contending nodes, $M = 3$, $N = 50$, $\gamma = 0.6$.

small latency and also scales well with respect to the number of contenders.

Fig. 5.11 gives a success probability comparison between our proposed MAC protocol and CDR [1], when the number of contending nodes varies between 2 and 50. To make a fair comparison, we note that adding one channel or slot to our system increases the packet overhead by the same amount as adding one slot to the CDR protocol. The number of channels, in our system, is fixed to 3. We would like to remark that the parameters used in our protocol are calculated by solving the optimization problem in (5.6) with the distribution in (5.1), when $N = 50$ and $\gamma = 0.6$ an thus, the protocol does not need to know about the number of contenders. It can be observed that our protocol performs much better in all scenarios, and its performance drops out at a much lower rate compared to CDR as we increase the number of contending nodes.

The effect of sensing errors on the average success probability is depicted in

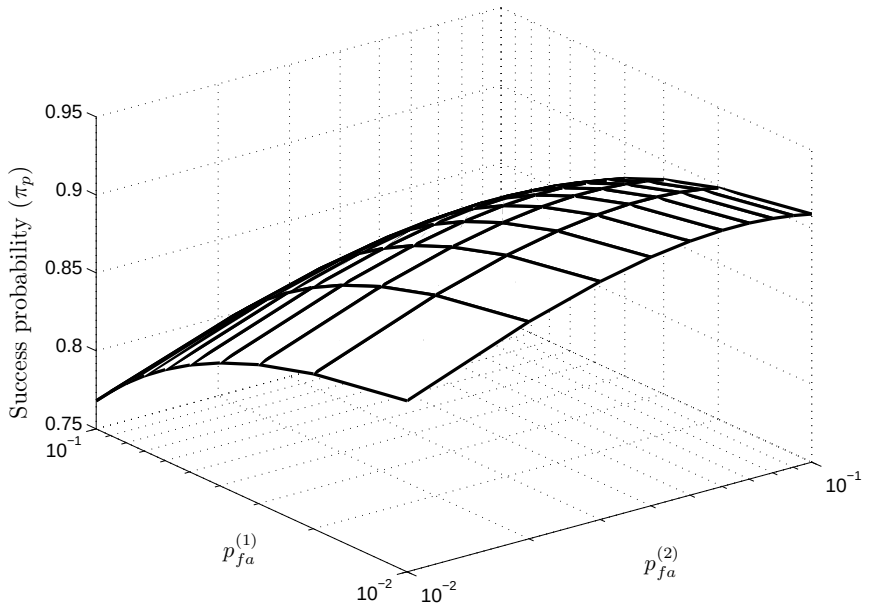

Figure 5.12: The average success probability versus false alarm errors, $N = 50$, $\gamma = 0.6$, $k = 6$, $M = 2$, $u = 10$.

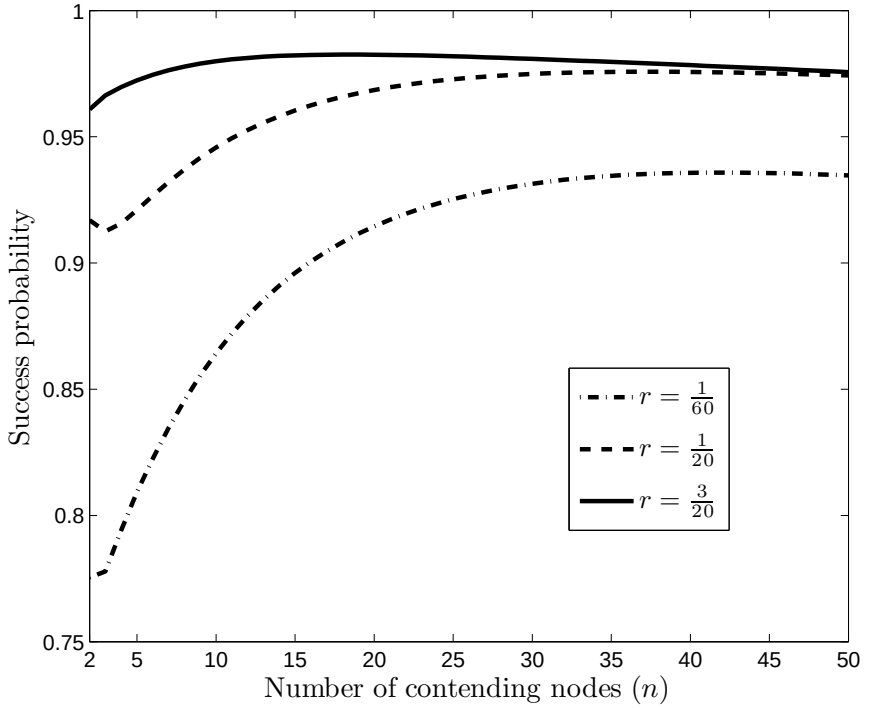

Figure 5.13: Success probability versus number of contending nodes for multiple values of r, where good channel is indexed 1, $k = 6$, $M = 2$, $N = 50$, $\gamma = 0.6$.

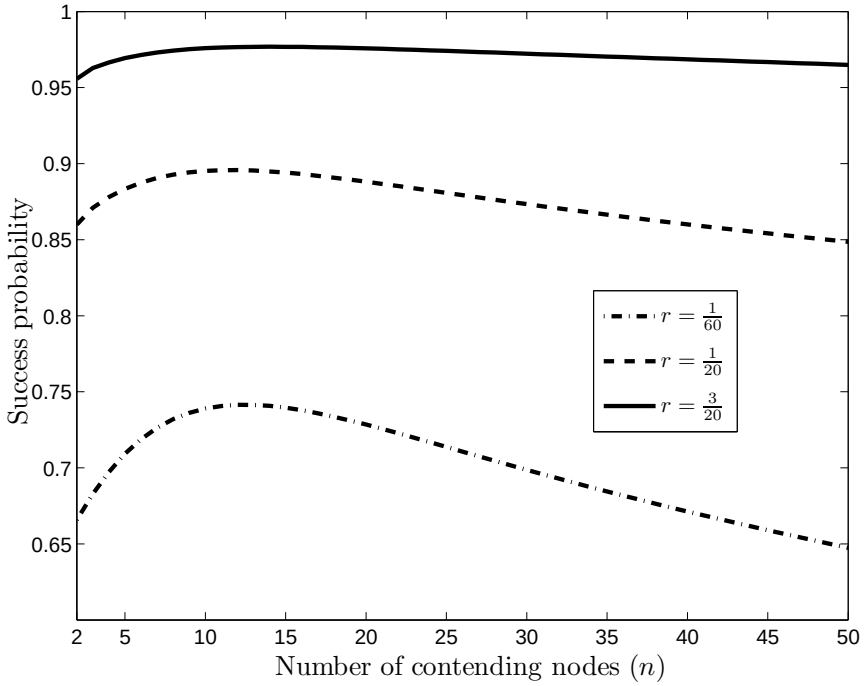

Figure 5.14: Success probability versus number of contending nodes for multiple values of r, where bad channel is indexed 1, $k = 6$, $M = 2$, $N = 50$, $\gamma = 0.6$.

Fig. 5.12. We consider the scenario where $k = 6$ slots and $M = 2$ channels are used in the system as it provides a high throughput according to the Fig. 5.5. The values of SNRs are set between -5dB to 5dB, and are chosen randomly in each channel. Note that each point in the figure represents the average probability of success as in (5.3), and is averaged over 1,000 runs. We also assume that the sensing module takes 20 samples to determine the presence or absence of the carrier. As can be seen, the success probability is sensitive to the false alarm errors on both channels, and there is an optimal point which maximizes the success probability. Next, we design a robust system by considering the carrier sensing errors. We plot the results for three cases correspond to $r = \frac{1}{60}, \frac{1}{20}, \frac{3}{20}$. Note that in all cases the packet length is fixed, and instead the number of samples taken from the received signal changes. There are $M = 2$ channels available in the system for contention, and assume the SNRs correspond to these channels are 5dB (good channel) and 0dB (bad channel).

Figs. 5.13-5.14 show the systems where the detector operating point is optimized on each channel with respect to the physical layer characteristics, and are correspond to the cases where the good channel is indexed as the first channel and vice versa, respectively. We can make the following observation. The success probability decreases when the bad channel is indexed 1. This happens since, according to (5.5), the receiver will receive the packet from the low-indexed channels with high probability, and a low SNR on the selected channel can degrade the performance of the collision resolution algorithm performed on that channel. Hence, we can shuffle the order of the channels in each transmission cycle to reduce the impact of the noise and fading on the MAC protocol performance.

5.5 Summary

In this chapter, we have introduced a random access MAC protocol based on the combination of time and frequency multiplexing. Nodes in the contention randomly select a frequency channel to perform channel contention in a number of slots. After that, the receiver samples the signal level on each frequency channel and stops on the first non-idle channel to receive the packet. We mathematically analyzed the performance of the proposed MAC protocol under both perfect and imperfect sensing. With numerical evaluations, we have verified our analysis and demonstrate the effectiveness of our MAC protocol. Our results show that the system demonstrates a good performance in terms of collision probability, system throughput, and delay. In this work, we have also considered that the system is not free from carrier sensing errors, and we have observed that a great care must be taken into account when designing such a system.

Chapter 6

Conclusions and Future Work

In this chapter, we first summarize the results and highlight the contributions of this thesis. Then, we propose possible future research directions.

6.1 Summary of Contributions

In this thesis, we focused on PLC systems employing carrier-sense-based MAC protocols for in-vehicle networks. Three contention-based MAC protocols were proposed and their performances were analyzed under imperfect carrier sensing. We then obtained optimum carrier sensing parameters to improve the MAC layer performance. In the following, we summarize the main contributions of the thesis.

- In Chapter 3, we have introduced a multi-carrier MAC protocol for in-vehicle PLC networks. The protocol employs a combination of time and frequency multiplexing to resolve the contention between nodes. We addressed physical layer related carrier sensing errors, i.e., false alarm and miss detection, and obtained the probability of successful transmission and time utilization as a function of these errors. To maximize the probability of successful transmission, we proposed a cross-layer approach where the average signal–to–noise ratio and sampling rate in each subcarrier were included in calculating the probability distribution that nodes use to randomly select subcarriers, and carrier sensing threshold that is being employed in each subcarrier.

- In Chapter 4, we have studied the effect of carrier sensing errors on the performance of a contention-based MAC protocol, called selective tournaments, well suited for in-vehicle power line communication. We obtained the network throughput and delay as a function of carrier sensing errors. Finally, numerical results were presented to demonstrate the sensitivity of the network throughput and delay with respect to the carrier sensing threshold.

- In Chapter 5, we have introduced a random access protocol, which consists of two key features: (i) a distributed channel selection policy that arbitrates packet transmission across different channels, and also provides robustness against interference and noise and (ii) a distributed collision resolution algorithm that allows each node to compete for the use of its selected channel. We have obtained the protocol-operational parameters that reduce the collision probability among senders. In addition, we have considered the impact of sensing errors on the performance of the proposed protocol, and analyzed the performance of the proposed protocol under the presence of sensing errors. We demonstrated the impact of the selection of the protocol parameters in determining the performance of the proposed protocol, and provided useful guidelines for developing a robust contention-based protocol for vehicular power line communication systems.

6.2 Suggestions for Future Work

In the following, we propose several interesting future research directions that are based on the work in this thesis.

1. **Developing a discrete-event simulator for the MAC layer of in-vehicle PLC network.** In this thesis, we have introduced and analyzed three MAC protocols for collision resolution in automotive environments. It is interesting to evaluate the performance of these protocols via simulations of the PHY and MAC layers. By doing this, we can also investigate the impact of carrier sensing errors on the performance of the MAC layer more accurately.

2. **Estimation of impulsive noise parameters using neural networks**. In Chapter 2, we introduced a simple impulse filter to mitigate the impulsive noise components from received signal. It is also possible to model the in-vehicle PLC noise with a Partitioned Markov Chain (PMC) [15]. One possible future research direction is to estimate the parameters of the PMC with a neural network. By doing so, it is possible to design a more robust communication system for in-vehicle PLC.

Bibliography

[1] O. Amrani and A. Rubin, "Contention detection and resolution for multiple-access power-line communications," *IEEE Trans. Veh. Technol.*, vol. 56, no. 6, pp. 3879-3887, Nov. 2007.

[2] E. Bassi, F. Benzi, L. Almeida, and T. Nolte, "Powerline communication in electric vehicles," in *Proc. IEMDC 2009*, May 2009, pp. 1749-1753.

[3] Y. Maryanka, "Wiring reduction by battery power line communication," in *Proc. IEE Seminar on Passenger Car Electrical Architecture*, Jun. 2000, pp. 8/1-8/4.

[4] M. Mohammadi, L. Lampe, M. Lok, M. Mirvakili, R. Rosales, and P. van Veen, "Measurement and transmission for in-vehicle power line communication," in *Proc. IEEE ISPLC 2009*, Dresden, Germany, Apr. 2009, pp. 73-78.

[5] M. Lienard, M. O. Carrion, V. Degardin, and P. Degauque, "Modeling and analysis of in-vehicle power line communication channels," *IEEE Trans. on Veh. Technol.*, vol. 57, no. 2, pp. 670-679, Mar. 2008.

[6] Y. Yabuuchi, D. Umehara, M. Morikura, T. Hisada, S. Ishiko, and S. Horihata, "Measurement and analysis of impulsive noise on in-vehicle power lines," in *Proc. ISPLC 2010*, Copacabana Rio de Janeiro, Brazil, Mar. 2010, pp. 325-330.

[7] V. Degardin, M. Lienard, P. Degauque, E. Simon, and P. Laly, "Impulsive noise characterization of in-vehicle power line channels," *IEEE Trans. Electromagn. Compat.*, vol. 50, no. 4, pp. 861-868, Nov. 2008.

[8] V. Degardin, M. Lienard, P. Degauque, and P. Laly, "Performances of the homeplug PHY layer in the context of in-vehicle powerline communications," in *Proc. IEEE ISPLC 2007*, Pisa, Italy, Mar. 2007, pp. 93-97.

[9] H. Urkowitz, "Energy detection of unknown deterministic signals," *Proc. IEEE*, vol. 55, pp. 523-531, April 1967.

[10] H. Poor, *An Introduction to Signal Detection and Estimation, 2Ed.* New York: Springer-Verlag, 1994.

[11] A. J. Efron and H. Jeen, "Detection in impulsive noise based on robust whitening," *IEEE Trans. Signal Processing*, vol. 42, pp. 1572-1573, June 1994.

[12] V. Namboodiri and A. Keshavarzian, "Alert: an adaptive low-latency event-driven MAC protocol for wireless sensor networks," in *Proc. IPSN2008*, St. Louis, Missouri, USA, pp. 159-170.

[13] J. Galtier, "Tournament methods for WLAN: analysis and efficiency," *Graphs and Algorithms in Communication Networks* (Springer), pp. 379-400, 2010.

[14] ISO 11898-1:2003, "Road vehicles—Controller Area Network (CAN)—Part 1: Data link layer and physical signaling," *ISO International Standard*, 2003.

[15] B. D. Fritchman, "A binary channel characterization using partitioned Markov chains," *IEEE Trans. Inform. Theory*, vol. 13, no. 2, pp. 221-227, Apr. 1967.

[16] K. Jamieson, H. Balakrishnan, and Y. Tay, "Sift: A MAC protocol for event-driven wireless sensor networks," in *Proc. EWSN 2006*, Zurich, Switzerland, Feb. 2006, pp. 260-275.

[17] S. Boyd and L. Vandenberghe, *Convex Optimization*, Cambridge, U.K.: Cambridge University Press, 2004.

[18] *CAN Specification, Version 2.0*, Stuttgart, 1991, R. Bosch GmBh, Std.

[19] A. Schiffer, "Statistical channel and noise modeling of vehicular DC-lines for data communication," in *Proc. IEEE VTC 2000-Spring*, Tokyo, Japan, May 2000, pp. 158-162.

[20] N. Taherinejad, R. Rosales, L. Lampe, and S. Mirabbasi, "Channel characterization for power line communication in a hybrid electric vehicle," in *Proc. ISPLC 2012*, Beijing, China, Mar. 2012, pp. 328-333.

[21] J.W. Chong, D.K. Sung, and Y. Sung, "Cross-layer performance analysis for CSMA/CA protocols: impact of imperfect sensing," *IEEE Trans. on Veh. Technol.*, vol. 59, no. 3, pp. 1100-1108, Mar. 2010.

[22] D. Fertonani and G. Colavolpe, "On reliable communications over channels impaired by bursty impulse noise," in *Proc. ISPLC2008*, Jeju Island, Korea, April 2008, pp. 357-362.

[23] M. Abramowitz and I. A. Stegun, Eds., *Handbook of Mathematical Functions with Formulas, Graphs, and Mathematical Tables.*, National Bureau of Standards Applied Mathematics Series 55, Washington, D. C.: U. S. Government Printing Office, 1964.

[24] N. Navet, Y. Song, F. Simonot-Lion, and C. Wilwert, "Trends in automotive communication systems," in*Proc. IEEE*, vol. 93, no. 6, pp. 1204-1224, Jun. 2005.

[25] T. Benzi, T. Facchinetti, T. Nolte, and L. Almeida, "Towards the power line alternative in automotive applications", in*Proc. WFCS2008*, Dresden, Germany, May 2008, pp. 259-262.

Appendix A

Probability Generating Functions

We will briefly introduce the definitions and notations related to probability generating functions. Generating functions provide a technique for dealing with sum of independent random variables. Let X be a discrete random variable taking values in the non-negative integers $\{0, 1, 2, \dots\}$ with $P(X = j) = p_j$. Upper case letters denote a random variable, while lower case letters denote a realization.

Definition

The probability generating function of the random variable X defined over non-negative integers, is given by the polynomial

$$G(z) = p_0 + p_1 z + p_2 z^2 + \cdots = \sum_{j=0}^{\infty} p_j z^j = E(z^X) \tag{A.1}$$

An important property of a probability generating function is that it converges for $|s| \leq 1$ since $G(1) = \sum_{j=0}^{\infty} p_j = 1$. The probability generating function can be used to derive the probability of the random variable, as well as its moments as

$$P(X = j) = p_j = \frac{1}{j!} \frac{d^j G(z)}{dz^j} \tag{A.2}$$